Geological Society, London, Special Publications Online First

The Late Triassic dinosauromorph *Sacisaurus agudoensis* (Caturrita Formation; Rio Grande do Sul, Brazil): anatomy and affinities

Max C. Langer and Jorge Ferigolo

Email alerting service	click here to receive free e-mail alerts when new articles cite this article
Permission request	click here to seek permission to re-use all or part of this article
Subscribe	click here to subscribe to Geological Society, London, Special Publications or the Lyell Collection
How to cite	click here for further information about Online First and how to cite articles

Notes

The Late Triassic dinosauromorph *Sacisaurus agudoensis* (Caturrita Formation; Rio Grande do Sul, Brazil): anatomy and affinities

MAX C. LANGER[1]* & JORGE FERIGOLO[2]

[1]*Departamento de Biologia-FFCLRP, Universidade de São Paulo, 14040-901 Ribeirão Preto, Brazil*

[2]*Museu de Ciências Naturais, Fundação Zoobotânica do Rio Grande do Sul, 90690-000 Porto Alegre, Brazil*

Corresponding author (e-mail: mclanger@ffclrp.usp.br)

Abstract: Silesauridae is an exclusively Triassic group of dinosauromorphs, knowledge on the diversity of which has increased dramatically in the last few years. Silesaurid relationships are still contentious, as a result in part of different homology statements, particularly regarding the typical edentulous mandible tip of these animals. One of the most complete silesaurids yet discovered is *Sacisaurus agudoensis* from the Caturrita Formation (Late Triassic: Norian) of Rio Grande do Sul, Brazil, represented by numerous isolated bones recovered from a single site. The anatomy of *S. agudoensis* is fully described for the first time here, and comparisons are provided to other basal dinosauromorphs. *S. agudoensis* is a small-bodied animal (less than 1 m in length) that possesses a dentition consisting of leaf-shaped crowns with large denticles in the carinae, a plesiomorphic propubic pelvis with an almost fully closed acetabulum, elongate distal hindlimbs suggesting well-developed cursorial ability, and a laterally projected outer malleolus in the tibia. All previous numerical phylogenies supported a non-dinosaur dinosauromorph affinity for Silesauridae, but the reanalysis of one of those studies suggests that a position within Dinosauria is not unlikely, with silesaurids forming the basal branch of the ornithischian lineage.

Since the discovery of *Silesaurus opolensis* from the Late Triassic of Poland (Dzik 2003; Dzik & Sulej 2007; Fostowicz-Frelik & Sulej 2010; Piechowski & Dzik 2010), various studies identified taxa possibly sharing a close affinity to that dinosauromorph, aiming at a better understanding of the diversity and phylogenetic relationships of the immediate sister-group to dinosaurs (Parker *et al.* 2006; Ezcurra 2006; Ferigolo & Langer 2007; Irmis *et al.* 2007*a*; Nesbitt *et al.* 2007, 2010; Small 2009; Brusatte *et al.* 2010; Peecook *et al.* 2011; Sulej *et al.* 2011; Kammerer *et al.* 2012). Part of this diversity was assembled within a group named Silesauridae (Langer *et al.* 2010; Nesbitt *et al.* 2010), the inclusivity and relationships of which have been debated. Most phylogenies agree on their non-dinosaur affinity, forming either a clade (Irmis *et al.* 2007*a*; Nesbitt *et al.* 2010; Brusatte *et al.* 2010; Nesbitt 2011) or successive outgroups to Dinosauria (Ezcurra 2006). On the contrary, a few other studies (Ferigolo & Langer 2007; Niedzwiedzki *et al.* 2009) argue for an ornithischian affinity for *S. opolensis* and some of its allies.

One of the best known silesaurids is *Sacisaurus agudoensis*, briefly described by Ferigolo & Langer (2007) based on dissociated elements recovered from a bone accumulation of Late Triassic age in south Brazil. Deeply nested within Silesauridae,

S. agudoensis was recently suggested to represent the sister-taxon to *Diodorus scytobrachion* from the Late Triassic Timezgadiouine Formation, Morocco (Kammerer *et al.* 2012). Silesaurids represent key taxa for understanding the patterns of character acquisition in the origin of dinosaurs either as non-dinosaur dinosauromorphs, filling the gap between dinosaurs and their forerunners, or as basal ornithischians, adding to the depauperate Late Triassic fossil record of the group. *S. agudoensis* is no exception and its anatomy is fully presented here, as parameters for future studies on dinosauromorph phylogeny.

Geological and palaeontological context

The continental Triassic beds of Rio Grande do Sul, south Brazil, are thought to have been deposited in tectonically controlled rift-like depocentres, limited to the southernmost portion of the intracratonic Chaco-Paraná Basin (Zerfass *et al.* 2004). Within the Mid-Late Triassic Santa Maria Supersequence, the Caturrita Formation (Andreis *et al.* 1980) corresponds to the highstand systems tract of Santa Maria 2 Sequence (Zerfass *et al.* 2003), which transitionally replaced the transgressive mudstones of the Alemoa Member, Santa Maria Formation. Some

authors suggest that this coarsening-upwards succession was deposited in a braided fluvial system during a period of decreasing humidity (Holz & Scherer 2000; but see Zerfass *et al.* 2003). Lithologically, the Caturrita Formation consists mainly of fluvial channel sandstones, but conglomerates and mudstones also occur locally. As a whole, the Santa Maria Supersequence has yielded plant (Guerra-Sommer & Cazzulo-Klepzig 2000; Crisafulli & Dutra 2009), invertebrate (Pinto 1956; Gallego 1996) and fish (Perez & Malabarba 2002) remains, but it is better known for its rich tetrapod fauna (Huene 1942; Barberena *et al.* 1985; Schultz *et al.* 2001; Langer *et al.* 2007). It was divided into at least three biostratigraphic units (Abdala *et al.* 2001; Lucas 2001; Soares *et al.* 2011*a*) ranging from Ladinian to Norian in age, but possibly earlier and later fossils have also been noticed (Langer *et al.* 2007).

All specimens described here were excavated from the same layer of a single locality (Fig. 1) in the northwestern outskirts (Av. Independência and Liberdade crossing) of Agudo, Rio Grande do Sul, Brazil (29°38′34′ S; 53°15′28′ W), the coordinates of which were erroneously given in Ferigolo & Langer (2007). The type-stratum consists of a 50-cm-thick layer of fine-grained sandstones full of isolated bones and mudstone pebbles, which

extended for about 3 m on a small outcrop that has been destroyed by human occupation. This seems to represent the kind of laterally discontinuous and poorly sorted deposits that typically mark the transition between the Alemoa Member mudstones below and the Caturrita Formation sandstones above (Andreis *et al.* 1980). Apart from the dinosauromorph remains, the layer has yielded only cynodont teeth. These include cheek-elements of *Riograndia guaibensis* and *Brasilitherium riograndensis* (Ribeiro *et al.* 2011), the presence of which implies correlation to the 'Riograndia Assemblage Zone' of Soares *et al.* (2011*b*) within the Caturrita Formation. Soares *et al.* (2011*a*) suggested a Norian age for that Assemblage Zone, which fits recent radioisotopic dates for the coeval Ischigualasto Sequence in NW Argentina (Martinez *et al.* 2011) and the 'Long Norian' interpretation of the Late Triassic timescale (Muttoni *et al.* 2004; Furin *et al.* 2006; Fraser & Sues 2011; Irmis *et al.* 2011; Olsen *et al.* 2011).

In addition, remains of medium-sized *Exaeretodon*-like traversodontids were also found in the type-locality. These include a single caniniform tooth found together with *Sacisaurus agudoensis*, and more complete elements (mandibles, isolated teeth and a postcranium) from a fine-grained sandstone layer below the type-stratum
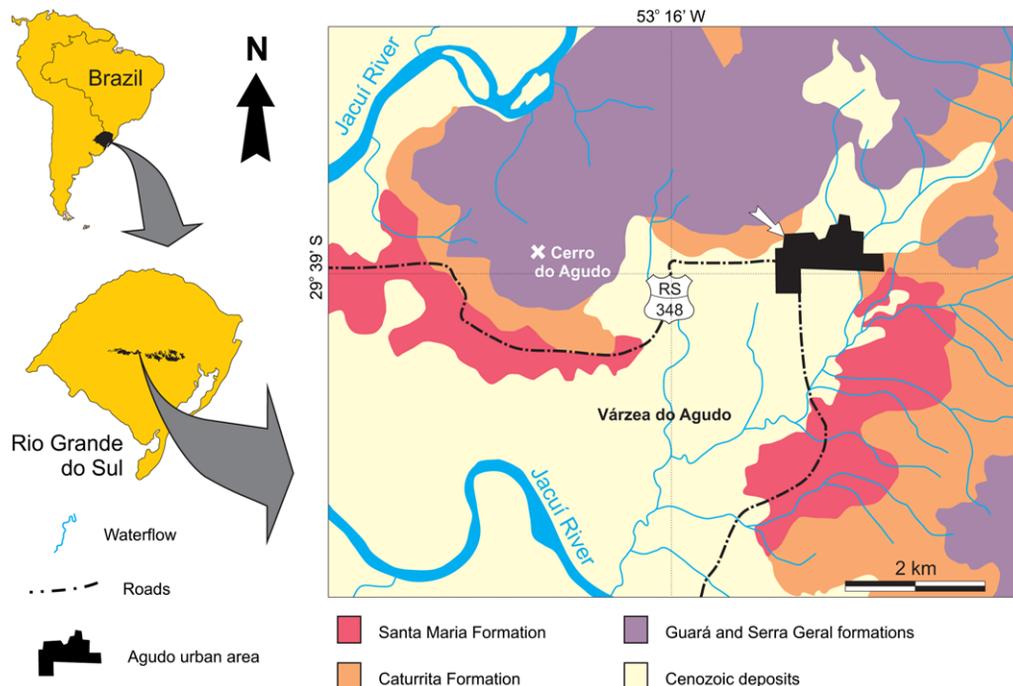
Fig. 1. Map of the Agudo area, Rio Grande do Sul, Brazil, showing the type-locality of *Sacisaurus agudoensis* (white arrow). Surface distribution of stratigraphic units based on Zerfass (2007).

(Ribeiro *et al.* 2011). The genus *Exaeretodon* is typical of the older *Hyperodapedon* Assemblage Zone (Langer *et al.* 2007), matching the abundance of similar forms in the lower strata of the type-locality.

Description

The assembling of dissociated fossil remains into single taxa has been common in Palaeontology (Heerden 1979; Chatterjee 1984, 1991; Benton *et al.* 2000; Fraser *et al.* 2002). This procedure is not beyond criticism, but more dubious if similar organisms are recognized in the same stratum/locus and if the assembled remains are excavated from different sites and/or associated in the absence of definitive diagnostic (autapomorphic) traits. Recent studies have employed an apomorphy-based approach as a surrogate for association (e.g. Irmis *et al.* 2007*a*; Nesbitt *et al.* 2010; Kammerer *et al.* 2012), which is also safer in specific taphonomic contexts (Rauhut 2005; Martinez & Alcober 2009). As for the dinosauromorph remains found in the bone accumulation dealt with here, the ilia and femora are the only duplicated elements with notable variations. The two recovered ilia (MCN PV10026, PV10100) are different in size and morphology, whereas two (MCN PV10007, 10008) of the known femora are significantly larger and also share distinctive anatomical traits. Most other recovered elements, including the holotype of *Sacisaurus agudoensis* (Ferigolo & Langer 2007), have relative sizes that better match those of the smaller ilium (MCN PV10100) and femora, but this is not the case of an ectopterygoid (Nesbitt 2011), a cervical vertebra (MCN PV10027) and a distal metatarsal I (MCN PV10040). These relatively larger elements are not referred to *S. agudoensis* here, and not included in the following descriptive accounts.

Evidently, not all elements referred to *Sacisaurus agudoensis* bear autapomorphies, but the matching morphology of the duplicated elements (lower jaws, teeth, vertebrae, pubes, ischia, femora, tibiae) suggests that the specimens described in the following sections correspond to individuals of a single taxon (a similar procedure is seen in Kammerer *et al.* 2012). Relative size differences are greater for some of the associated elements (vertebrae, metacarpals, phalanges), but they all fall within a broad 50% variation range relative to the preserved long bones (femora/tibiae). Despite sharing similar preservation, the overlapping of skeletal parts attributed to *S. agudoensis* (e.g. there is a most peculiar preservation of over 30 nearly identical right femora) shows that they correspond to numerous animals. Indeed, the lack of articulation precludes the association of bones to a single individual (expect for two likely matching right tibia/fibula pairs). Unless explicitly mentioned, descriptive accounts are valid for all duplicated bones.

Skull bones

The better maxilla recovered (MCN PV10050; Fig. 2a, c) lacks portions of the rostral margin and the tip of the caudal ramus. It was not freed from the matrix, and only its external surface is accessible. The dorsal ramus seems not caudally inset, but continuous to the rostral margin of the bone. It extends dorsally and slightly caudally, but its pinched tip is more caudally bent, suggesting that it was covered by the nasal. The rostral margin of the bone is concave, likely for the articulation of the premaxilla. The antorbital fossa excavates the caudal and especially the dorsal ramus of the maxilla, forming large external and internal antorbital fenestrae. It occupies about one-third of the rostrocaudal breadth of the base of the dorsal ramus, and tapers dorsally. It is also not very deep, lacking the rostral apertures typical of various dinosaurs (Witmer 1997; Rauhut 2003; Tykoski 2005; Butler *et al.* 2008; Martinez *et al.* 2011). However, a small hemispherical pocket with two internal subsidiary depressions excavates the rostroventral corner of the fossa. It penetrates some distance into the body of the dorsal ramus, and may correspond to the promaxilary fenestra/fossa (Rauhut & Fechner 2005; Tykoski 2005; Yates 2005; Ezcurra 2007; Sereno 2007; Cabreira *et al.* 2011; Martinez *et al.* 2011). The antorbital fossa extends for about one-quarter of the preserved rostrocaudal length of the maxillary caudal ramus. It is not markedly excavated, but more dorsoventrally expanded at the rostral part, tapering caudally. As a result, the ventral margin of the external antorbital fenestra is subparallel to the ventral margin of the maxilla. A row of at least four foramina pierce the caudal maxillary ramus and bulging areas occur at the level of the sockets for the larger and/or fully erupted teeth, separated by subtle excavations. On its medial side, the rostral margin of a fragmentary maxilla (MCN PV10091) preserves a short/plate-like palatal ramus.

A left postorbital (MCN PV10051) is also imbedded in matrix, with only the lateral surface visible (Fig. 2b). It has well-developed rostral, caudal and ventral rami, and a subtle excavation bordering the supratemporal fenestra extends along the latter two. Between the rostral and ventral rami, a typical convexity marks the orbital border as also recognized in many basal dinosauromorphs (Haubold 1991; Sereno 1991; Langer 2004; Tykoski & Rowe 2004; Cabreira *et al.* 2011; Martinez *et al.* 2011). Because of their tapering shape, the
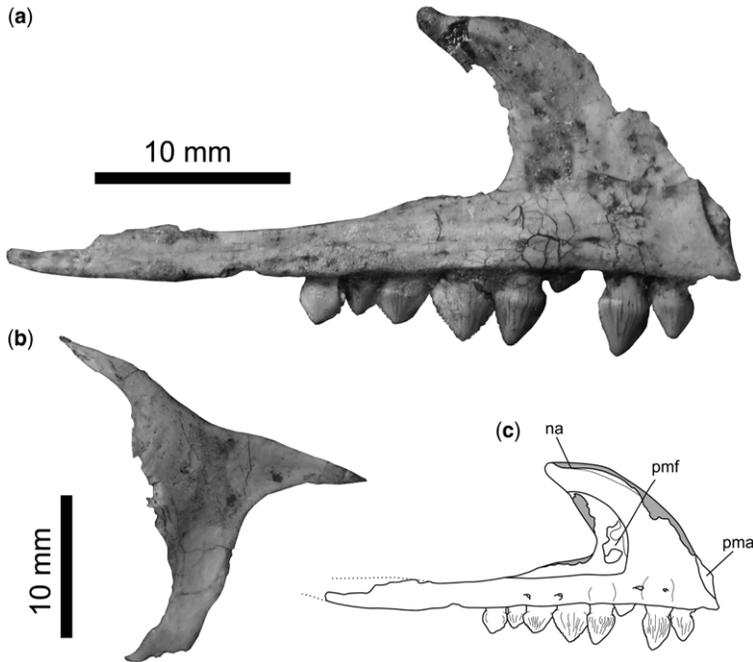
Fig. 2. *Sacisaurus agudoensis*, lateral view of isolated skull bones: **(a)** right maxilla (MCN PV10050); **(b)** left postorbital (MCN PV10051); and **(c)** respective interpretative drawing of (a). Reconstructed parts in grey. *Abbreviations*: na, nasal articulation; pma, premaxilla articulation; pmf, promaxillary fossa.

tips of the rostral and caudal rami probably slotted into the external surfaces of the frontal and squamosal, respectively; the ventral ramus seems to overlap the ascending ramus of the jugal rostrally. A subtle longitudinal groove extends along the caudal ramus.

Mandible

In addition to more fragmentary lower jaw remains (e.g. MCN PV10045, PV10046), the rostral portions of six hemimandibles (Figs 3–6) have been recovered (MCN PV10040, PV10041, PV10042, PV10043, PV10048, PV10061). A length variation of about 20% was observed based on the distance (possible to measure in four of the specimens) between the rostral tip of the jaw and the eighth alveolus. No clear sutures are observed in those fragments, but their edentulous rostral portion is described separately in the last three paragraphs of this section. The remaining tooth-bearing part of the jaw is composed only by the dentary, which is a nearly straight, lateromedially flattened bone. It is somewhat deeper caudally and its rostral portion is slightly concave laterally. The ventral margin is mostly convex, but slightly concave at the rostral end. This is mirrored by the dorsal margin of the bone, somewhat convex rostrally but more concave caudally. The external surface of the dentary shows

depressed areas at the level of the empty alveoli and/or not fully erupted teeth and is traversed by a shallow longitudinal groove, dorsal to which lies a series of nutrient foramina. These do not correspond to the tooth position, that is, there is no larger foramen for each tooth or erupted tooth. The depressed areas, and possibly also the groove, may be taphonomic in origin due to the collapse of bone surface in less robust areas of the jaw (not internally supported by fully developed tooth roots). At the medial surface of the bone, the narrow Meckelian channel extends rostrocaudally along its ventral edge. It bears a sharp dorsal margin and its rostral part is narrower and slightly dorsally displaced, finishing about the level of the caudal margin of the third tooth position where an ovoid pocket is seen (PV10043). This is also known in *Silesaurus opolensis* (GG 111 361/27) but it is not clear if it leads to a foramen as in *Asilisaurus kongwe* ('f' in Nesbitt *et al.* 2010), although these seem to be present at the dorsorostral and ventrocaudal margins ('f' in Figs 4a, 5a & 6b). Striations on the rostral margin of MCN PV10048 (Fig. 5a), which lacks the toothless tip of the jaw, suggests that the dentary takes part on the symphysis.

In the hemimandibles exposed in medial view, the toothless rostral portions are either missing (MCN PV10048) or connected to the rest of the
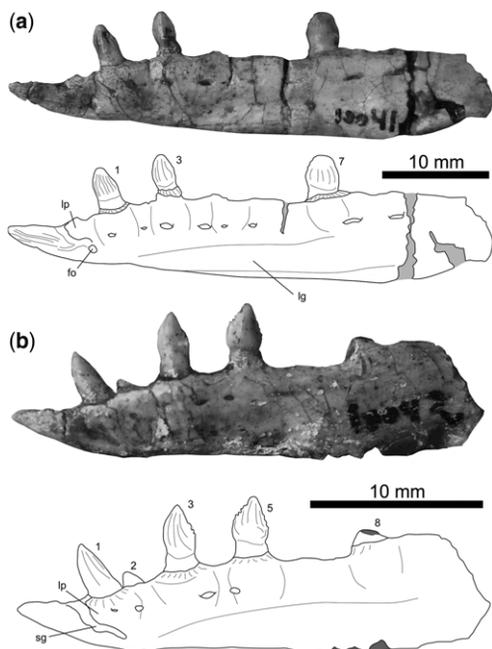
Fig. 3. *Sacisaurus agudoensis*, partial right hemimandibles in lateral view with respective interpretative drawings: **(a)** holotype (MCN PV10041) and **(b)** MCN PV10042. Broken areas in grey. *Abbreviations*: fo, foramen; lg, longitudinal groove; lp, lateral projection; sg, sigmoid groove. Teeth are numbered according to their inferred positions.

Fig. 4. *Sacisaurus agudoensis*, partial right hemimandibles with respective interpretative drawings: **(a)** MCN PV10043 in medial view and **(b)** MCN PV10061 in lateral view. Abbreviations as in Figure 3 plus: dg, dorsal groove; f, fomamina; mch, meckelian channel; op, ovoid pocket; sr, symphiseal ridge; vg, ventral groove. Teeth are numbered according to their inferred positions.

jaw by continuous bone surface (MCN PV10040, PV10043). In specimens exposed in lateral view, the degree of association of the symphyseal/rostral area to the caudal part of the hemimandible is variable. In some of them (MCN PV10040, PV10042, PV10061), this is marked by a deep 'sigmoid groove' (see Irmis *et al.* 2007*b*) which extends caudoventrally from the dorsal margin of the jaw until near its ventral margin. The computerized tomography (CT) image of MCN PV10040 indicates that a possible ventral extension of that groove in fact corresponds to a fracture in the bone (Fig. 6c). If the rostral portion of the hemimandible is interpreted as a separate element (Ferigolo & Langer 2006), the 'sigmoid groove' would demarcate its caudal edge.

The 'rostral element' of *Sacisaurus agudoensis* was identified as the ornithischian predentary by Ferigolo & Langer (2007), an often admitted neomorphic apomorphy of that group. Although we consider this a possibility, its full implications are beyond the aims of this work. Described as a separate element, its lateral outline is subtriangular with free dorsal and rostroventral margins, and bound

Fig. 5. *Sacisaurus agudoensis*, partial left hemimandible (MCN PV10048) in medial view with respective interpretative drawing. Abbreviations as in Figures 3–4.
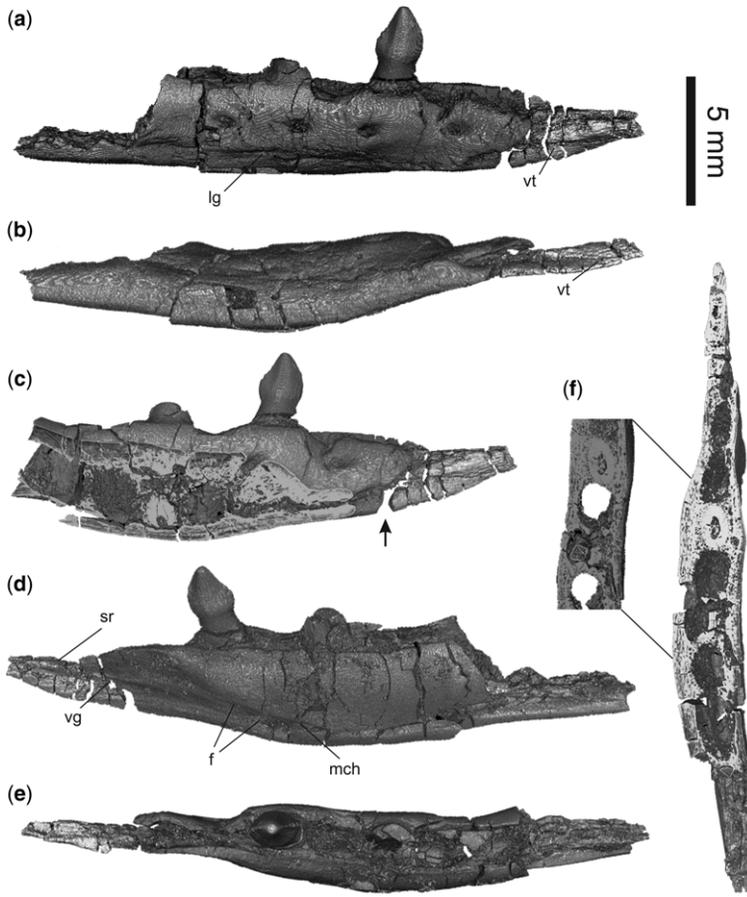
Fig. 6. *Sacisaurus agudoensis*, partial right hemimandible (MCN PV10040) reconstructed from micro-CT data in **(a)** lateral; **(b)** ventral; **(c)** lateroventral (with parasagittal section); **(d)** medial; and **(e)** occlusal views; **(f)** transverse section of the upper portion, with detail on a more ventral level. Arrow indicates fracture in the bone. Abbreviations as in Figures 3–4 plus: vt, ventral trough.

dorsocaudally by the 'sigmoid groove'. It has a straight to slightly convex dorsal margin, a convex rostroventral margin and a slightly dorsally directed pointed rostral tip. Its lateral surface is striated (MCN PV10040, PV10041) and depressed relative to the tooth-bearing area. This resembles the jaw of *Silesaurus opolensis* (Dzik 2003), the edentulous rostral tip of which is also depressed in relation to more caudal structures, suggesting the presence of a keratinous cover. The caudoventral portion of the 'rostral element' of *Sacisaurus agudoensis* extends under a subrectangular projection ('lp' in Figs 3–4 & 6) that emanates from the lateral surface of the dentary. It slightly overlaps the rostral half of the sigmoid groove, giving its characteristic (sigmoid) outline in lateral view. This also occurs in *Silesaurus opolensis* (ZPAL AbIII/437/1), and a possibly equivalent structure is seen in ornithischians

with an underdeveloped dorsocaudal process of the predentary (Butler *et al.* 2008; Zheng *et al.* 2009, fig. 1e; Norman *et al.* 2011).

The caudal margin of the depressed rostral area of the holotype jaw of *Sacisaurus agudoensis* is pierced by a foramen ('fo' in Fig. 3a). This is not clear in the other referred hemimandibles, but the CT scan of MCN PV10040 (Fig. 6c) revealed that the 'sigmoid groove' leads caudally to a tunnel entering the bone. The holotype foramen leads rostrally to a subtle bifurcating trough, resembling those associated with the 'anterior dentary foramen' of ornithischians (Sereno 1991; Sereno & Dong 1992). Its ventral branch (also seen in MCN PV10040; 'vt' in Fig. 6a, b) is subparallel to the ventral margin of the jaw, whereas the dorsal branch extends dorsorostrally in the direction of a concavity at the dorsal margin of the bone, passing rostral

to the subrectangular projection of the dentary. The path between the dorsal branch and the foramen corresponds to the 'sigmoid groove'. The subtleness of that structure may be due to the more extensive ossification of the holotype, which is the largest lower jaw exposed in lateral view, and may represent an older individual. A similar configuration of grooves is seen in the depressed 'beak' of *Silesaurus opolensis*, but although vascular structures were described on its caudal margin (Dzik 2003; p. 563) the rostroventrally extending furrow is more reminiscent of an anchor surface for the corneous beak (ZPAL Ab III/437/1), as also suggested by striations in MCN PV10040.

In medial aspect, the 'rostral element' of *Sacisaurus agudoensis* bears an oblique longitudinal ridge ('sr' in Fig. 4a, 6) that extends ventrocaudally from near the tip of the jaw, forming the dorsal margin of a corresponding groove ('vg' in Fig. 4a). In MCN PV10043, the ridge faints caudal to the level of the first tooth, reaching the 'oval pocket' as an inconspicuous fold. The groove is not considered an extension of the Meckelian channel. In fact, although somewhat aligned, these structures are separated by an oblique bulge ventral to the 'ovoid pocket' (MCN PV10043) and the rostral groove is broader/shallower than the Meckelian channel. In addition, striations are seen on the ventral margin of the groove as well as on a subtriangular excavation between the ridge and the dorsal margin of the jaw, which leads to a more dorsally placed groove ('dg' in Fig. 4a). A similar pattern is seen in *Silesaurus opolensis* (ZPAL AbIII/437/1), in which the entire medial surface of the beak is covered by symphyseal striations. Both longitudinal depressions, as well as the ridge between them, are therefore related to the symphyseal articulation and the entire 'rostral element' was medially articulated with its counterpart.

Dentition

Upper and lower jaw teeth of *Sacisaurus agudoensis* are similar in most aspects. The more complete maxilla bears eight obvious tooth positions, all except the third of which are occupied by nearly fully erupted (sixth and seventh teeth) or fully erupted teeth. The third position was also originally occupied by an erupted tooth, which left its impression in the bearing matrix. Its loss, possibly during collection/preparation, revealed the apex of a medial replacing tooth. One extra tooth position may occur both rostral and caudal to the preserved elements, suggesting a complete series of about 10 teeth, which did not reach the caudal end of the bone. The dentary with the highest number of tooth positions (MCN PV10061) indicates the presence of 12 elements, but the total number in a

complete jaw was probably about 15. Teeth are not markedly inset from the lateral margin of both maxilla and dentary (Figs 7a, b), and the available information (MCN PV10050, PV10061) suggests that teeth are larger at the central to caudocentral portions of the dental series, reducing in size both rostraly and caudally. Kammerer *et al.* (2012) suggested that a significant decrease in tooth size along the rostral portion of the dentary is apomorphic for the clade composed by *S. agudoensis* and *Diodorus scytobrachion*, but this is clear only in MCN PV10043 and PV10061, as further considered in the discussion below.

There is some variation in shape between more rostral teeth and those from the middle to caudal part of the series. Crown bases are all expanded, but especially mesiodistally and in more caudal teeth. Accordingly, in specimens with adjacent teeth preserved (MCN PV10048, PV10050), an *en echelon* arrangement (the distal margin of each tooth laterally overlapping the mesial portion of the one behind) is only clear among caudal elements. Isolated teeth preserved with their roots (MCN PV10052, PV10053, PV10060) reveal a constriction marking the crown–neck boundary, with the crown base slightly broader (mesiodistal and labiolingual) than the main part of the root (Figs 7g, h). These are usually twice the length of the crown and either cylindrical or somewhat mesio-distally compressed. Crowns are all labio-lingually compressed but to a lesser degree in more rostral teeth, as well as at their base, which remains convex (bulbous) both lingually and labially. The lingual convexity is always stronger, forming a basal cingulum in various specimens (MCN PV10053, PV10056, PV10058, PV10060) where a semi-lunar pit can occur due to wearing (MCN PV10058, PV10060). In some specimens (MCN PV10040, PV10048, PV10054a), it is possible to see the lingual bulbous base leading to a longitudinal smooth ridge that extends apically at the centre of the lingual surface of the crown (Figs 5 & 7f), a subtler version of which is also seen in the labial surface (MCN PV10053, Fig. 7k). This is flanked by smooth depressions, which more roughly excavate the rounded crown base forming mesial and distal lips. The longitudinal ridge corresponds to the 'middle ridge' Hopson (1975; 'central primary ridge' of Butler *et al.* 2008) identified in heterodontosaurids, whereas the lips are equivalent to the mesial and distal ridges of Butler *et al.* (2008), as also known in various other basal ornithischians (Thulborn 1970; Colbert 1981; Butler *et al.* 2006). In addition, subtle longitudinal striations are seen in most teeth of *Sacisaurus agudoensis* (e.g. seventh tooth of MCN PV10061), but these are not as marked as in some *Silesaurus opolensis* teeth (Dzik 2003, fig. 5i).
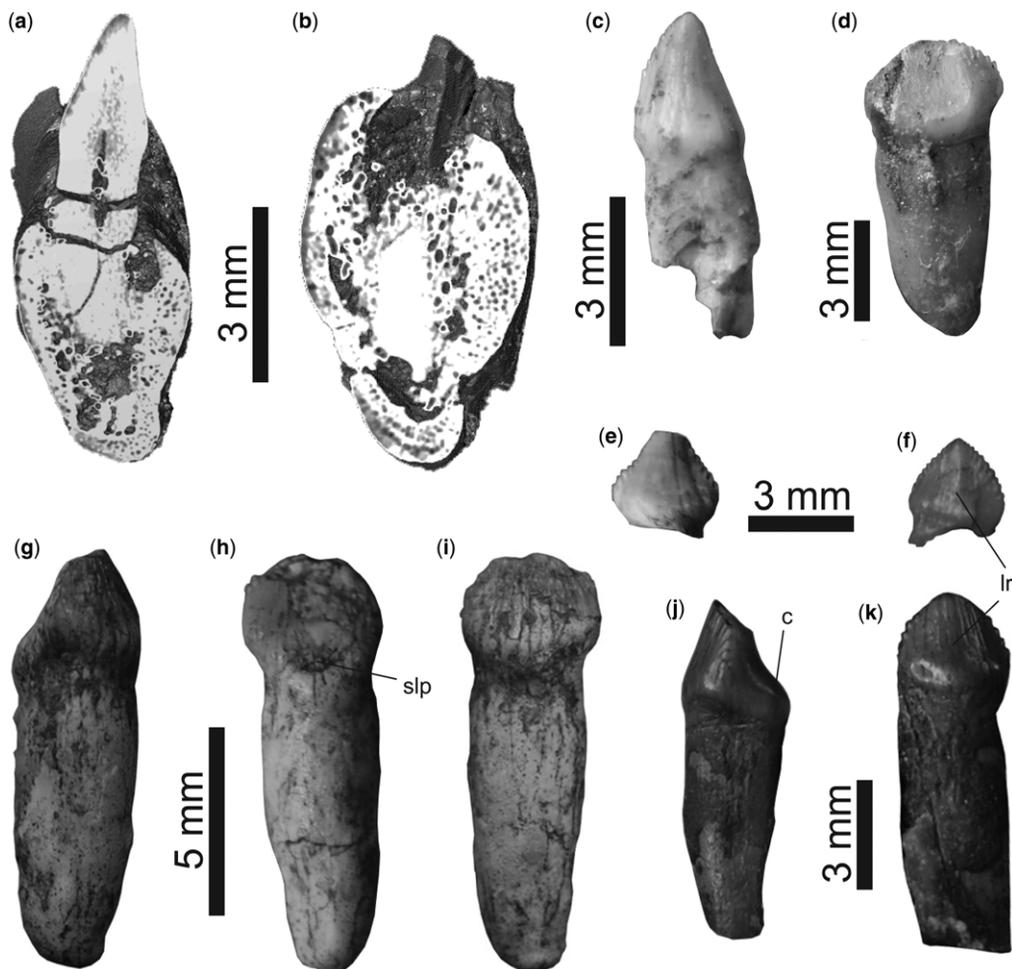
Fig. 7. *Sacisaurus agudoensis* teeth. Cross-sections of MCN PV10040 from micro-CT data, at the level of the **(a)** third and **(b)** fifth teeth. Photographs of **(c)** MCN PV10057a in labial/lingual view; **(d)** MCN PV10058 in lingual view; **(e)** MCN PV10056 in lingual view; **(f)** MCN PV10054a in lingual view; MCN PV10060 in **(g)** distal/mesial, **(h)** lingual and **(i)** labial views; MCN PV10053 in **(j)** distal/mesial and **(k)** lingual views. *Abbreviations*: c, cyngulum; lg, longitudinal ridge; slp, semi-lunar pit.

Tooth crowns of the rostral part of maxilla and especially dentary are more leaf shaped (labial/lingual view), that is: slender, mesial and distal margins forming a sharper apex; mesial margin entirely convex and distal margin convex at the base and concave apically, so that the apex points slightly distally. Otherwise, more caudal teeth tend to have a subtriangular shape, that is: more mesio-distally expanded at the base, mesial and distal margins convex at the base and nearly straight apically, forming an apex angle of almost 90°. An unusual isolated tooth crown (MCN PV10056) is especially expanded mesio-distally at the base, so that both of these margins are convex at the base

and concave apically, with a pinched labiolingual outline (Fig. 7e). Rostral and caudal tooth crowns also differ in mesial/distal views, the former showing less expanded basal portions. Their apical portions are convex labially and concave lingually, and slightly curved in that direction (MCN PV10057). Caudal teeth have more expanded bases and straight lingual and labial margins towards the apex. The former is more extensive, due to the more bulbous base (cingulum) on the respective side. Despite retaining the subtriangular shape of larger elements, smaller crowns positioned at the caudal end of the tooth series (MCN PV10050, PV10061) are usually also less bulbous at the

base. Kammerer *et al.* (2012) draw attention to the 'canted' shape of some *Sacisaurus agudoensis* teeth. Indeed, the first preserved tooth of MCN PV10043 and PV10061 and, to a certain degree of the holotype, is shaped as if its crown was displaced mesially with a less marked distal expansion of the base. One isolated tooth (MCN PV10057) has a somewhat similar outline, and the significance of this feature is dealt with in the Discussion.

Sacisaurus agudoensis teeth bear denticles in both the mesial and distal keeled margins but their number, size and positions are variable. Usually, denticles are less evident on the mesial margin and at the apical portion, but this may be related to a higher degree of wearing and to the smaller denticle size in the tooth apex (as seen in MCN PV10048). In most specimens the count ranges from three to eight denticles on the mesial margin and from four to seven on the distal margin, but a particularly well-preserved and unworn tooth (MCN PV10054) has up to 14 denticles on each margin. In a newly erupted unworn tooth (MCN PV10095) there are six and four denticles on the distal and mesial carinae, respectively. Denticles are smaller in more rostral teeth, forming oblique angles to the long axis of the crown, whereas those of more caudal elements are larger and almost parallel to the long axis of the tooth.

The teeth of *Sacisaurus agudoensis* were deeply implanted into the jaw bones, as indicated by long-rooted isolated teeth and the CT scan of MCN PV10040, but the labial wall of the dentary is slightly more developed than the lingual (Figs 4a & 6a,b); this set of traits is somewhat halfway between the classical thecodont/subthecodont insertion types. Nesbitt *et al.* (2010) suggested that some silesaurids (including *S. agudoensis*) had teeth 'ankylosed to the dentary'. Indeed, gross inspection of the surface texture in the tooth-bearing areas of the lower jaw of *S. agudoensis* allows the recognition of a gutter in the dentary, into which teeth are attached by a somewhat different kind of bony material (see also Figs 6a, b). This fills the space between teeth, as well as between these and the neighbouring walls. Such a distribution resembles that of alveolar bone in the genus *Platecarpus* (Caldwell *et al.* 2003), the teeth of which also bear bulbous mass of cementum at the base. A similar 'collar' of radiating trabeculae is seen at the base of some teeth of *S. agudoensis* (especially in MCN PV10048), *Silesaurus opolensis* (ZPAL AbIII/361/26) and the Hayden Quarry *Silesaurus*-like form (Irmis *et al.* 2007*a*), suggesting that these were not typically thecodont, that is, fixed in the alveoli by fibrous connective tissue (Osborn 1984). Such an implantation better fits the definition of ankylosed thecodonty (Edmund 1969; Motani 1997) or ankylothecodonty (Chatterjee 1974), as

more often recorded among basal archosauro-morphs. In rhynchosaur ankylothecodonty (Benton 1984; Cabreira 2004), typical reptilian replacement is absent, a probable synapomorphy of derived members of the group (Dilkes 1998). It is symptomatic that (regardless of their small size) not a single isolated rhynchosaur tooth has ever been found in the upper Santa Maria Formation, although the group accounts for 90% of its tetrapod fossil record (Langer *et al.* 2007). The recovery of isolated teeth referred to *Sacisaurus agudoensis* indicates that ankylosis is either absent, less extreme than that of rhynchosaurs or restricted to later stages of dental development (see Sues 2003; p. 638). This is congruent with the characterization of ankylosis given by Osborn (1984, pp. 556–557) which allows replacement processes, and with the record of attachment bone surrounding teeth that are normally replaced in various fossil reptiles (Small 1997; Sues 2003; Modesto & Sues 2004; Säilä 2009).

The CT scan of MCN PV10040 revealed the fifth (broken) tooth in replacement process. Its root is not as long as that of the third tooth and a dental germ is present at the bottom of a chamber medial to the tooth (Fig. 6f). The presence of resorption pits/embayments in some jaw elements of *Sacisaurus agudoensis* (MCN PV10043, PV10048, PV10095) further emphasizes this substitution pattern. These are seen in the interface of the lingual wall of the dentary gutter and the 'attachment bone' that surround the teeth, forming a rounded excavation on the latter. This is also seen in various fossil reptiles (Edmund 1960; Ewer 1965; Gauffre 1993; Gower & Senikov 1997; Small 1997; Caldwell *et al.* 2003; Sues 2003), including other silesaurids (Irmis *et al.* 2007*a*; Kammerer *et al.* 2012) and ornith-ischians (Colbert 1981; Crompton & Attridge 1986; Thulborn 1992; Butler 2010). Equivalent perforations in the tooth-bearing bones occur closer to the erupted teeth (Martin 1981; Norell & Hwang 2004) and between neighbouring interdental plates in basal saurichians (Barrett *et al.* 2005; Yates 2005; Kutty *et al.* 2007; Allain & Aquesbi 2008; Martinez 2009), at the base of which they form 'replacement foramina' in large carnivorous archo-saurs (Bonaparte 1981; Gower 1999; Galton 2005; Benson *et al.* 2008; Sereno & Brusatte 2008; Bru-satte *et al.* 2009). Accordingly, interdental plates are here interpreted as outgrowths of the attach-ment bone that meet one another apical to the resorption pits.

The distribution of fully grown dentary teeth in *Sacisaurus agudoensis* has a seemingly regular pattern of intercalation with alveoli that are empty or bearing non-erupted teeth. The CT scan of MCN PV10040 revealed fully erupted third and fifth teeth and five unfilled spaces, completing seven

tooth positions, while the holotype has fully erupted first, third, fifth (broken) and seventh teeth and an unfilled space caudal to each, completing eight tooth positions. MCN PV10042 has fully erupted first, third and fifth teeth separated by unfilled spaces (the first with the apex of a replacement tooth), and the eighth (broken) tooth neighboured by two rostral and one caudal vacant spaces. A similar condition is seen in MCN PV10043 with fully erupted first, third, fifth (broken), eight and tenth tooth, completing 11 preserved positions. MCN PV10061 slightly diverges from the last pattern with erupted first, fourth and seventh teeth separated by two empty positions, and ninth and eleventh teeth neighboured by one unfilled space both caudally and rostrally. Regardless of these differences, it seems that an intercalated pattern is prevalent in *S. agudoensis*. This is common for archosaurs (Edmund 1960; Chatterjee 1978, 1985; Colbert 1981, 1989; Welles 1984; Gow *et al.* 1990; Walker 1990; Gower & Sennikov 1997; Jalil & Peyer 2007; Upchurch *et al.* 2007) and may reveal a substitution process with 'Z-spacing' equal to two tooth positions. On the contrary, the more complete maxilla and one of the dentaries (MCN PV10042) do not show the intercalated pattern but instead a continuous series of eight and six erupted teeth, respectively.

Vertebral column

Thirteen isolated vertebral elements were recovered from the bone accumulation of *Sacisaurus agudoensis*. They fit the general morphology of archosaur vertebrae, but most lack unambiguous dinosauromorph apomorphies. Indeed, their referral to *S. agudoensis* must be treated with caution, especially for the purpose of character coding in phylogenetic analyses. Except for a cervical vertebra (MCN PV10027), all vertebral elements recovered from the type-locality of *S. agudoensis* match the relative size of the other remains attributed to the taxon, and are described below. Nonetheless, their association is justified only by the absence of other archosaurs in the site and their distinction from cynodont vertebrae, the only other tetrapod group recorded in the locality.

The only recovered neck element corresponds to an atlantal intercentrum (MCN PV10032; Fig. 8a–d). It has a crescentic craniocaudal outline, deeply concave on its dorsal margin and convex ventrally. This convexity encompasses the ventral and lateral surfaces, which bear a markedly rugose texture. The bone is craniocaudally constricted at the centre, which matches a flattening on its ventral margin. Both cranial and caudal surface bear thickened ventral borders; while the former is excavated the latter is heterocoelous, that is, dorsoventrally convex and lateromedially concave. The dorsal surface bears two subtriangular excavations (apices facing medially) mirrored in each side. The trunk segment is represented by two badly preserved vertebrae. MCN PV10235 is a badly crushed (craniocaudally flattened) neural arch, the cranial surface of which is still imbedded in matrix. Its transverse processes are elongated and the hyposphene projects over the caudal aperture of the neural channel. MCN PV10088 is an isolated platycoelous centrum, the articulations of which are broader than deep. It is constricted in the middle, but lacks a ventral keel. The lack of parapophyseal articulations suggests that it belongs to the caudal part of the trunk.

A set of nine caudal vertebrae has been recovered: one from the proximal part of the tail, four from its mid-distal portion and four from its distal end. The centrum of the proximal caudal vertebra (MCN PV10028; Fig. 8e–f) is as long as it is high and constricted at the middle. Both articulations are expanded, slightly excavated, and higher than broad, but the distal has more thickened borders. The ventral margin has a subtle keel and distal articulation area for the haemal arch. There is no sign of the neurocentral suture, and the transverse processes extend laterally from the ventrolateral portion of the neural arch as slightly distally expanded and dorsally arched structures. Their distal margins are incomplete, but there is no sign of a separate 'parapophyseal' articular facet. Subtle ridges emanate from the transverse processes in the direction of the proximal and distal upper corners of the centrum, forming a transversally elongate pit below each process. The neural channel is broader than high proximally, but narrower distally, and the short prezygapophyses project from the proximal margin of the neural arch. The equally short postzygapophyses are raised on the neural spine, which projects dorsally and slightly distally as a thin sheet of bone.

Vertebrae from the mid-distal portion of the tail (MCN PV10097, PV10230, PV10234, PV10336) have lateromedially compressed (especially at the middle) and proximodistally elongated centra (Fig. 8g). Their lateral surfaces are excavated by an axially elongated shallow fossa below each transverse process. The articulations are higher than broad and slightly excavated. Facets for the haemal arches form slightly expanded proximal and distal corners. The concave ventral margin of the centra bears a subtle midline groove flanked by a pair of longitudinal raised areas (MCN PV10097). The transverse processes are relatively short and proximo-distally narrow, extending laterally and slightly distally from the neurocentral joint. They are surrounded by subtle ridges that extend towards the zygapophyses, proximal and distal
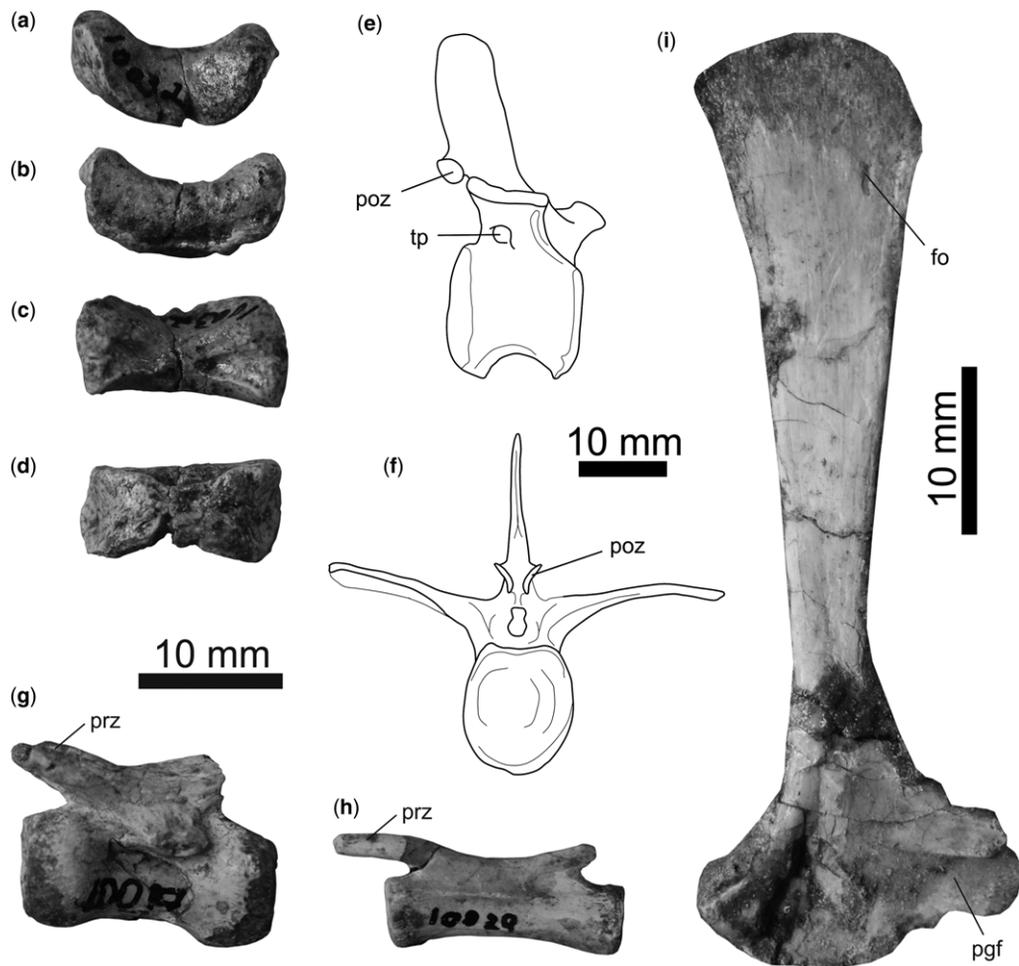
Fig. 8. *Sacisaurus agudoensis*, vertebrae and pectoral girdle elements. Atlantal intercentrum (MCN PV10032) in (**a**) cranial, (**b**) caudal, (**c**) dorsal, and (**d**) ventral views; interpretative drawing of a proximal caudal vertebra (MCN PV10028) in (**e**) lateral and (**f**) caudal views; (**g**) middle (MCN PV10017) and (**h**) distal (MCN PV10029) tail vertebra in lateral views; (**h**) left scapula (MCN PV10033) in lateral view. *Abbreviations*: fo, foramen; pgf, preglenoid fossa; poz, postzygapophyses; prz, prezygapophyses; tp, transversal pit.

upper corners of the centrum. The neural channel is higher than broad, and its proximal aperture is flanked by short prezygapophyses that extend only slightly over the proximal margin of the centrum. No distal portion of the neural arch is entirely preserved, but the neural spine reaches the level of the distal margin of the transverse process as a faint ridge between the proximal extensions of the postzygapophyses. Centra of the distal-most caudal vertebrae (MCN PV10029, PV10031, PV10082, PV10090) are elongated and lateromedially constricted in the middle. The concave ventral surface bears a midline groove, flanked by subtle collateral ridges. Proximal and distal articulations are rounded

and slightly concave. No vestige of a neural spine remains, and the dorsal margin of the neural arch is flattened. The transverse processes are reduced to proximodistally elongated lateral ridges. The postzygapophyses are short, but the long prezygapophyses are inferred to extend over about one-quarter of the proximally adjacent centrum. In the best-preserved element (Fig. 8h), the prezygapophyses lack their proximal tips but project proximal to the centrum at a distance equivalent to 23% of the centrum length.

Several rib fragments were recovered in the bone accumulation of *Sacisaurus agudoensis*. A right rib (MCN PV10079) exposed in caudal view appears to

belong to the cervical series. The equally developed capitulum and tuberculum are medially connected by a caudally excavated sheet of bone. In some dinosaur cervical vertebrae (Huene 1926; Galton 1974; Colbert 1989) this lamina forms a cranial spine, but this is not possible to determine here. The tuberculum is incomplete and somewhat flattened, whereas the rod-like capitulum is ventrally bowed. Their bases form a nearly right angle and lead to a relatively thin shaft continuous to the capitulum. Although incomplete, the tapering shaft seems to extend caudally as a short and nearly straight element. A right trunk rib (MCN PV10078) is exposed in caudal view, showing a less-developed internal lamina. The capitulum is straighter and longer, whereas the incomplete shaft is continuous to the short tuberculum. The dorsally convex margin of the latter matches the external bowing of the shaft that typically shapes the chest, but a dorsal depression is formed between them. An isolated proximal portion of a left rib (MCN PV10085) probably belongs to a more caudal part of the truck series. The medial surface between the incomplete heads is filled by a well-developed lamina. The capitulum is more plate-like, whereas the shaft curves away from a stouter tuberculum. MCN PV10086 is probably from the rear end of the trunk. Capitulum and tuberculum are not divided by a notch but discrete at the same plane, forming a continuous arch with the rest of the rib. The only recovered haemal arch (MCN PV10089) has a short shaft that is caudally inclined and axially expanded at its distal part. The proximal portion of the arch bridges the haemal channel dorsally, and forms a wedge-shaped proximal articulation.

Pectoral girdle and limb

An isolated scapula, imbedded in the matrix and exposed in lateral view (Fig. 8i), and two probable appendicular bones are the only pectoral elements recovered from the bone accumulation of *Sacisaurus agudoensis*. The scapular blade is lateromedially flattened (MCN PV10033). It reaches its minimal craniocaudal breadth near the base, and expands dorsally with nearly straight cranial and caudal margins. The dorsal margin is composed of unfinished bone, but seems to be rounded. The lateral surface of the blade lacks any distinctive structure, apart from a possible perforating foramen on its dorsocranial portion. The ventral body of the scapula includes a more robust caudal part and a lateromedially flattened and cranially projected scapular prominence. At the caudoventral corner, the caudally facing scapular glenoid forms an angle of about $45°$ to the long axis of the blade. It is lateromedially flattened (possibly a preservation bias), but broader ventrally than dorsally.

The laterally concave ventral third of the scapular prominence forms the preglenoid fossa (Welles 1984; Langer *et al.* 2007), the dorsal limit of which is marked by a sharp craniocaudally elongated ridge. Although nearly in the same position, this ridge differs from the preglenoid ridge of various dinosaurs (Sereno 1993; Langer *et al.* 2007) which are broader and reach the dorsal margin of the scapular prominence. On the contrary, a laterally concave plate-like bone expansion occurs dorsal to the ridge in MCN PV10033, as also seen in *Silesaurus opolensis* (ZPAL AbIII/361). The dorsal margin of the scapular prominence forms an angle of about $100°$ to the main axis of the scapular blade, whereas its ventral margin seems less ventrally projected than that of more caudal portions of the bone. Hence, although not well preserved, the scapular articulation to the coronoid appears to be sigmoid in outline.

Two badly preserved long bones may represent humerus and ulna. The probable left humerus (MCN PV10076) has its cranial surface still covered in matrix and is not easily photographed. It is a straight, elongated (99.80 mm) rod-like element, with slightly expanded proximal (15.45 mm) and distal (10.15 mm) portions. The proximal expansion is more marked towards the lateral side, which bears an elongated depression on the caudal surface also seen in specimens of *Silesaurus opolensis* (ZPAL AbIII/452). This is opposite to the deltopectoral crest (not visible), but does not seem to be well expanded cranially. The ulna (MCN PV10238) is badly crushed and lacks its distal end. The proximal portion is expanded, with a poorly developed olecranon process. Its medial surface is traversed by a longitudinal groove, right caudal to a medial expansion of the cranial surface. The proximal outline is subtriangular, with craniolateral (radius tuber) and caudolateral corners leading to longitudinal ridges that extend distally. The cranial ridge reaches the proximal margin of the bone, whereas the caudal element is more distally restricted. They delimit the flat lateral surface of the proximal ulna. If the forelimb elements of *Sacisaurus agudoensis* belong to a similar-sized animal as the more abundant hindlimb bones, the humerus would be almost as long as the femur and the epipodium not much shorter than the humerus (the incomplete ulna is 75 mm long).

Pelvic girdle

An isolated left ilium (MCN PV10100), left pubes (MCN PV10023, PV10024) and right (MCN PV10025) and left (MCN PV10237) ischia from the bone accumulation are tentatively referred to *Sacisaurus agudoensis*. The more complete bones (MCN PV10023, PV10025, PV10100) are of

nearly equivalent size, and assembled together in Figure 9. The ilium is visible both laterally and medially but lacks the dorsal margin and ischiadic peduncle; whereas the pubic peduncle, most of the acetabulum, the base of the preacetabular ala and most of the postacetabular ala are preserved. In lateral view, the pubic peduncle expands towards a convex pubic articulation. In distal view, this is elliptical in outline, broader at the ventral margin. The supraacetabular crest projects over the acetabulum for more than half the depth of that structure. It extents along the pubic peduncle as a fainter ridge, but does not reach the pubic articulation. Caudoventral to that, a sharp border ('acrb' in Fig. 8b) separates the peduncle from the recessed acetabular wall. The latter is not entirely preserved, but the ventral margin of its cranial part (which is articulated to the pubis) is convex, indicating either a fully closed acetabulum similar to *Marasuchus lilloensis* (PVL 3870) or a sigmoid margin as seen in *Silesaurus opolensis* (ZPAL AbIII 404/1) and some dinosaurs, for example *Saturnalia tupiniquim* (Langer 2003) and *Guaibasaurus candelariensis* (Langer *et al.* 2011). As typical of basal dinosauromorphs, a blunt 'iliac preacetabular ridge' (Langer 2003) extends from the dorsocranial margin of the supracetabular crest towards the incomplete preacetabular ala. Judging from the size and position of its base the ala is much reduced, somewhat fitting the morphology of silesaurid ilia (Dzik 2003; Irmis *et al.* 2007a). The postacetabular ala is also incomplete, lacking its caudal margin. Its lateral surface is crossed by a ridge that corresponds to the brevis shelf. This is not continuous to the supracetabular crest, but extends dorsocaudally from above the acetabulum. Its incomplete caudal portion overhangs slightly, marking the dorsal border of the brevis fossa. Ventral to the shelf, the postacetabular ala is covered by sediment and its ventral margin is elusive. The concave dorsal outline of the ilium is a taphonomic signature seen in a number of archosaurs, for example *Bromsgroveia*

walkeri (Galton & Walker 1996), *Effigia okeeffeae* (Nesbitt 2007), *Silesaurus*-like form (Irmis *et al.* 2007a), *Guaibasaurus candelariensis* (Langer *et al.* 2011) and *Silesaurus opolensis* (ZPAL AbIII/907/8, 907/6). This may have been filled by a more extensive but narrow and laterally excavated iliac lamina, as seen in *Silesaurus opolensis* (ZPAL AbIII/361). The sacral rib articulations are the most noticeable features of the medial surface of the ilium. Based on the comparison to *Silesaurus opolensis* (ZPAL AbIII/907/6), the ovoid articulation facet caudally adjacent to the preacetabular embayment of the ilium may correspond to the articulation of the first sacral rib, whereas the oblique ridge extending along the postacetabular ala was probably enveloped by the rib/transverse process (Bittencourt *et al.* 2012) of the third sacral vertebra.

Both pubes (Figs 11 & 12) are incomplete distally, although MCN PV10024 lacks a larger portion of the shaft. The overall bone morphology and articulation pattern clearly indicate a propubic pelvis construction. The proximal pubic body is composed of a robust dorsal portion, the caudal process (Langer 2003) and the obturator plate. These form rather complex proximal margin and articulation to the other pelvic bones. The slightly convex articulation facet for the iliac pubic peduncle of MCN PV10024 has an ovoid (dorsomedially to ventrolaterally elongated) proximal outline (Fig. 11a). Its ventral limit is formed by a shallow transverse groove (also seen in *Silesaurus opolensis*; ZPAL AbIII/361) which separates the main iliac articulation from the cranial margin of the acetabulum ('af' in Sullivan & Lucas 1999; 'pai' in Langer 2003) that received the femur, and also enters somewhat onto the lateral surface of the bone. Indeed, if present, the pubic contribution to the medial acetabular wall would be formed solely by a laminar dorsal extension of the caudal process of the bone, as seen in *S. opolensis* (ZPAL AbIII/361). An inconspicuous ischio-acetabular groove (Sullivan & Lucas 1999; Langer 2003) is seen in lateral view, separating the main part of the pubic body from the caudal process. Although the iliac articulation projects somewhat medially, the medial surface of the proximal body is almost evenly concave. On the contrary, two conspicuous ridges extend along its external surface, separated by a broad sharp-edged groove ('dg' in Figs 11 & 12). One marks the dorsal limit of the body and diminishes towards the shaft. Its implicit, distal continuation is represented by the limit between the more robust lateral portion of the shaft and its medial lamina. The second forms a proximodistally elongated 'pubic tubercle' (*sensu* Hutchinson 2001), continues distally as the lateral margin of the shaft, but is proximally bifurcated into two branches at the level
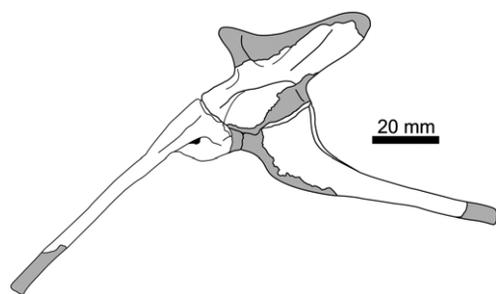
Fig. 9. *Sacisaurus agudoensis*, reconstruction of the pelvic girdle. Ilium and ischium at the indicated scale; pubis reduced to 80%. Missing parts in grey.

of the obturator foramen. The dorsal branch extends until the base of the main iliac articulation, right dorsal to the subtriangular depression that marks its ventral limit (MCN PV10024). The ventral branch forms a broader pillar ('pil' in Figs 11 & 12) that supports the femoral articulation in the pubic acetabular margin, dorsal to the ischio-acetabular groove. Ventral to that, the caudal process and the obturador plate form the rounded lower margin of the proximal pubis. The latter probably contacted the ischium (Fig. 9), but is not completely preserved in any specimen of *Sacisaurus agudoensis*. Distal to that, the obturator plate extends ventrally as a nearly vertical sheet of bone, pierced by a single obturator foramen. At the level of the 'pubic tubercle' the plate twists (Fig. 11c) mediodorsally, is aligned

orthogonal to the sagittal plane and extends distally as the horizontal medial lamina of the pubic shaft. Accordingly, the shaft is formed of a more robust lateral border and a thin medial lamina.

Both ischia are incomplete distally, but whereas MCN PV10237 is visible from all sides (Fig. 13b–d) only the medial surface of MCN PV10025 was freed from the matrix. The proximal body of the ischium bears a large dorsocranially facing iliac articulation and a ventrally expanding obturator plate. However, the ventral margin of the plate as well as the pubic articulation are lacking in both specimens. In dorsal view, the proximal portion of MCN PV10237 arches outwards, but its obturator plate is medially convex and the partial shaft nearly straight; whereas MCN PV10025 forms an inner
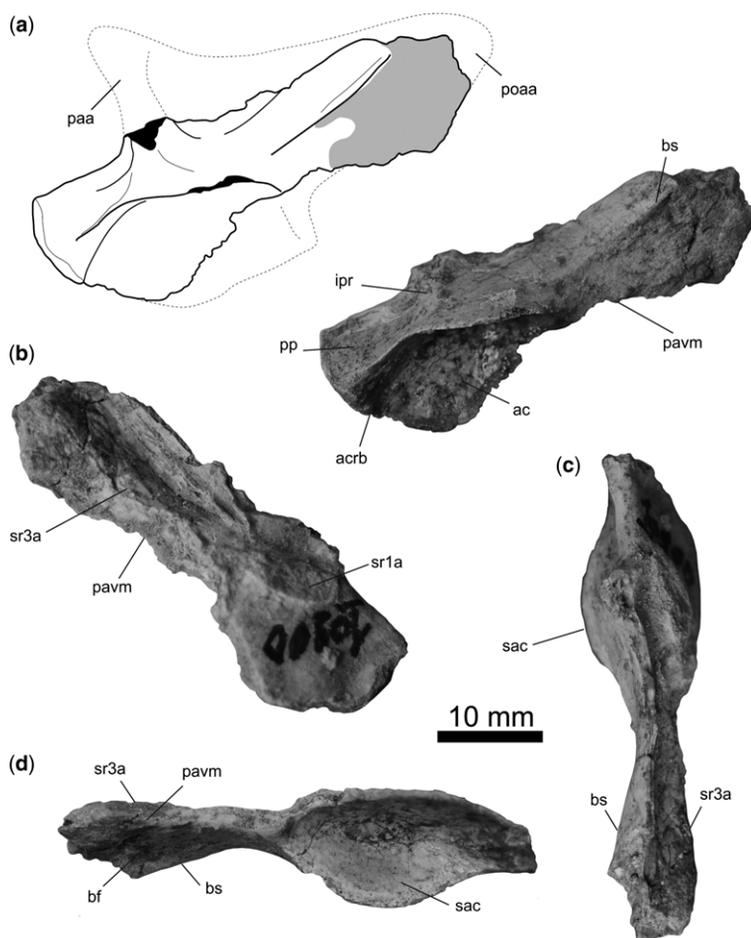
Fig. 10. *Sacisaurus agudoensis*, left ilium (MCN PV10100) in **(a)** lateral (with respective interpretative drawing); **(b)** medial; **(c)** dorsal; and **(d)** ventral views. Reconstructed outline in dotted lines; broken surfaces in black, sediment cover in grey. *Abbreviations*: ac, acetabular wall; acrb, acetabular cranial border; bf, brevis fossa; bs, brevis shelf; ipr, iliac preacetabular ridge; paa, preacetabular ala; pavm, ventral margin of postacetabular ala; poaa, postacetabular ala; pp, pubic peduncle; sac, supracetabular crest; sr1a, articulation of first sacral rib; sr3a, articulation of third sacral rib.
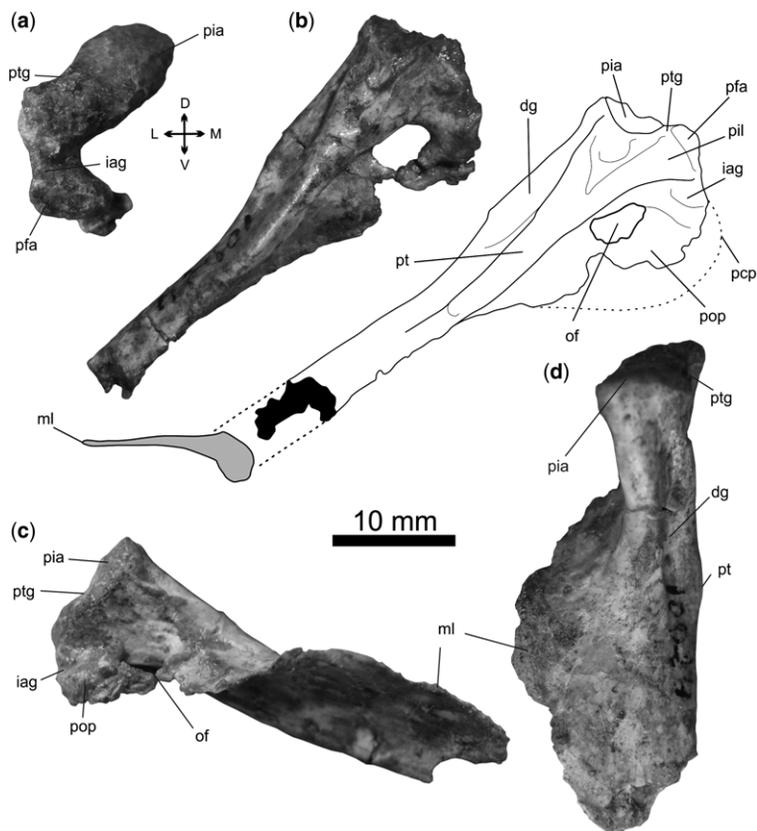
Fig. 11. *Sacisaurus agudoensis*, left pubis (MCN PV10024) in **(a)** proximal (directions indicated); **(b)** lateral (with respective interpretative drawing); **(c)** medial; and **(d)** dorsal views. Reconstructed outline in dotted lines; broken surface in black, cross-section of the broken distal end in grey. *Abbreviations*: dg, dorsal groove; iag, ischio-acetabular groove; ml, medial lamina; pfa, pubic femoral articulation; of, obdurator foramen; pcp, caudal process of the pubis; pia, pubic iliac articulation; pil, pubic pillar; pop, pubic obturator plate; pt, pubic tubercle; ptg, pubic transverse groove.

arch for its entire length. The caudoventral portion of the obturator plate bears medial striations for the symphyseal articulation. Distal to that (MCN PV10025), the bone continues conjoined to its pair along the entire length of the shaft. The obturator plate of MCN PV10237 is apparently more distally extensive. This notion results from the preservation of a smaller portion of the bone of a larger individual, and the ischial shaft is here interpreted as mostly rod-like (as preserved in MCN PV10025). A longitudinal groove ('dg' in Fig. 13) extends along the dorsolateral margin of the ischial body, bound laterally and medially by ridges, the medial of which ('dmr' in Fig. 13) forms the sharp dorsomedial corner of the bone. Along the ischial shaft, this set of structures is medially displaced. The lateral ridge extends as the dorsolateral corner of the bone and the dorsomedial ridge as the inner edge of a mediodorsally facing narrow platform

('dp' in Fig. 13), which is the distal extension of the longitudinal groove. This slightly overhangs another groove ('sg' in Fig. 13) that extends along the ischial symphysis, as seen in *Silesaurus opolensis* (ZPAL AbIII/363). This resembles the longitudinal excavation that makes the twisted ischial shaft of some ornithischians faintly concave dorsomedially (Butler 2005, 2010). Indeed, structures equivalent to the dorsal ridges and groove have also been described for those dinosaurs (*Lesothosaurus diagnosticus*, Butler 2005, fig. 4; *Eocursor parvus*, Butler 2010, fig. 13).

Femur

The bone accumulation of *Sacisaurus agudoensis* includes a most unusual assemblage of 36 femoral fragments (Table 1), encompassing a minimal number of 29 individuals. Fourteen femora are
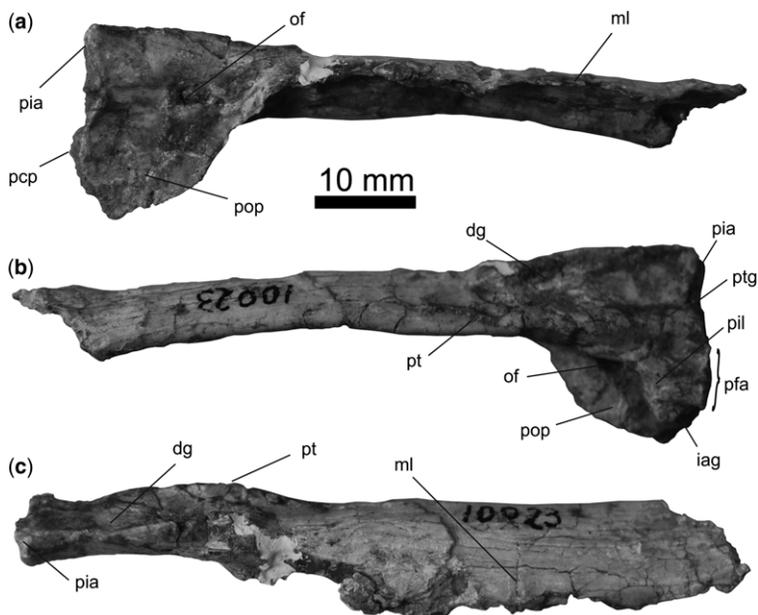
Fig. 12. *Sacisaurus agudoensis*, left pubis (MCN PV10023) in **(a)** medial; **(b)** lateral; and **(c)** dorsal views. Abbreviations as in Figure 11.

virtually complete, and only one element was assignable to the left side. They range from nearly 90 mm to about 110 mm long and are nearly identical in most details, except for preservational features associated with differential compression that modified the shape of the bones (especially their proximal and distal articulations). The femur is cranially bowed for its entire length, but sigmoid if seen in lateral/medial views (Fig. 14). This is given by the medial and lateral curvatures of, respectively, the proximal and distal portions of the bone, somewhat enhanced by the inturning and slight medial expansion of the head. Accordingly, the proximal articulation is subparallel to the distal in cranial/caudal views, and does not lean medially as in basal theropods (Raath 1977; Rowe 1989; Nesbitt *et al.* 2009*a*). In proximal/distal views, the angle formed by the long axis of the head and the intercondilar line is subject to preservation biases. It is minimal in craniocaudally flattened femora (MCN PV1010), reaches up to 60° in lateromedially flattened elements (MCN PV1013), but is of about 45° in most apparently less-deformed bones (Fig. 15). Equally, the proximal outline of the femur is variable (Figs 15, 16a, b) because of postmortem deformation (flattening). It is subtriangular in most specimens, with marked medial, caudolateral and cranial ('clt' in Fig. 16) corners, the latter corresponding to the 'anterolateral tuber' (Irmis *et al.* 2007*a*; Nesbitt 2011). Both craniomedial and

craniolateral margins are straight, but the latter is considerably longer. The longest caudal margin bears two concavities separated by a protuberance, all of which extend slightly distally along the medial surface of the bone. The medial concavity and the protuberance respectively correspond to the 'ligament sulcus' and 'medial tuber' ('posteromedial tuber' of Nesbitt 2011) as defined by Novas (1996), variously referred to in recent studies of basal dinosauromorphs such as *Saturnalia tupiniquim* (Langer 2003), '*Syntarsus*' *kayentakatae* (Tykoski 2005), *Eucoelophysis baldwini* (Ezcurra 2006), *Coelophysis bauri* (Nesbitt *et al.* 2007), *Dromomeron romeri* and *D. gregorii* (Nesbitt *et al.* 2009*b*), *Staurikosaurus pricei* (Bittencourt & Kellner 2009) and *Eocursor parvus* (Butler 2010). The lateral concavity is in the position of the facies articularis antitrochanterica of Langer (2003, 2004), Nesbitt *et al.* (2007), Barrett *et al.* (2008) and Butler (2010), *non* Forster *et al.* (2009), i.e. 'trochanteric fossa' of Novas (1996) and Ezcurra (2006). Yet, differently from the condition in basal dinosaurs such as *Herrerasaurus ischigualastensis* (Novas 1993), Snyder Quarry coelophysoid (Nesbitt *et al.* 2007) and *Eocursor parvus* (Butler 2010), it expands only slightly onto the proximal surface of the head. Indeed, in some specimens of *Sacisaurus agudoensis*, the proximal and caudal surfaces of the femur converge in that area forming a nearly right-angled corner. This is the case
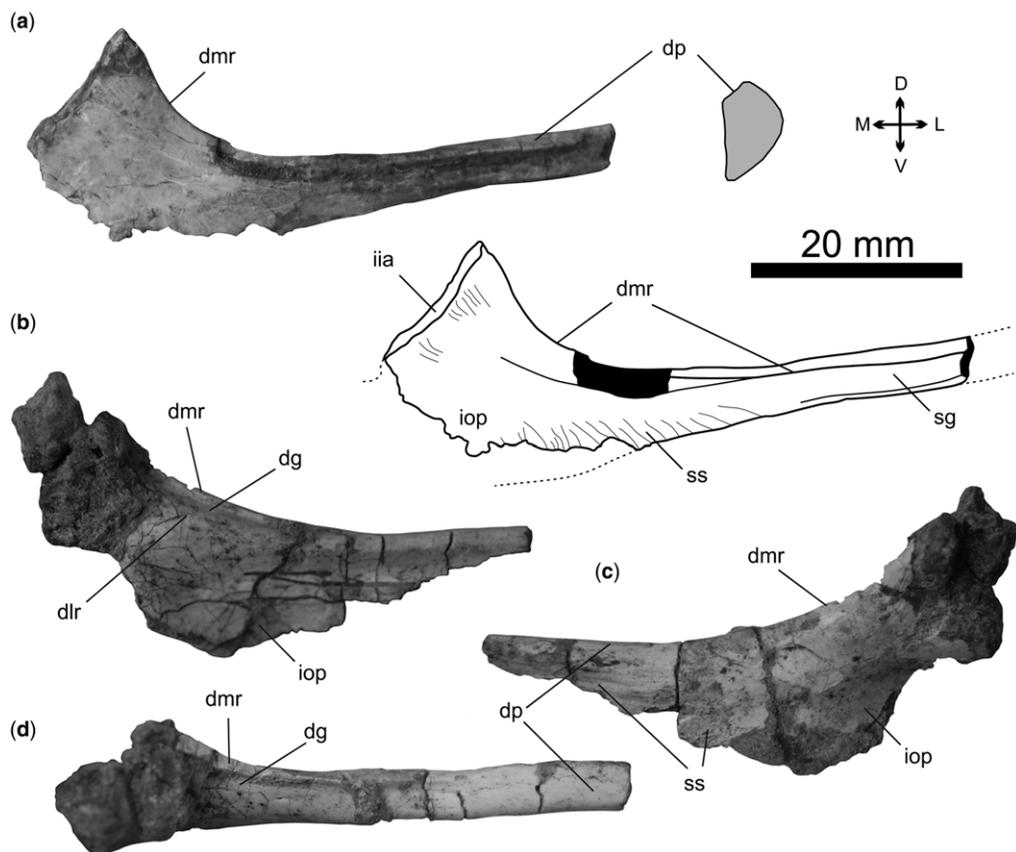
Fig. 13. *Sacisaurus agudoensis*, ischia: **(a)** right ischium (MCN PV10025) in medial view with respective interpretative drawing; left ischium (MCN PV10237) in **(b)** lateral, **(c)** medial and **(d)** dorsal views. *Abbreviations*: dp, dorsal platform; dg, dorsal groove; dlr, dorsolateral ridge; dmr, dorsomedial ridge; iia, ischial iliac articulation; iop, ischial obturator plate; sg, symphiseal groove; ss, symphiseal striations. Reconstructed outline in dotted lines; broken surface in black; cross section of the shaft in grey (with directions indicated).

for a particular femur (MCN PV10019; Ferigolo & Langer 2006), the 'medial tuber' of which is completely lacking. The proximal outline of this bone is evenly concave caudally, resembling the condition in *Lesothosaurus dianosticus* (NHMUK RUB17). In any case, all recovered femora of *S. agudoensis* have the medial tip of the head ('caudal lip') slightly projected caudally, but not to the extent seen in some dinosaurs (Tykoski 2005; Ezcurra 2006). In addition, an irregular longitudinal groove ('pg' in Fig. 16) extends along the proximal articulation, as typical of many dinosauromorphs (Langer 2003; Ezcurra 2006; Bittencourt & Kellner 2009; Butler 2010; Nesbitt *et al.* 2010).

The caudal surface of the femoral head is nearly flat, although a subtle ridge ('mr' in Fig. 16) extends distally from the 'medial tuber', flanked by a pair of equally subtle grooves. There is no clear evidence of

either an obturator (Raath 1990) or caudolateral (Langer 2003; Nesbitt *et al.* 2007; Bittencourt & Kellner 2009) ridge. *Sacisaurus agudoensis* has the 'notch' ventral to the femoral head considered typical of silesaurids (Irmis *et al.* 2007a; Nesbitt *et al.* 2010), but this seems to represent the result of two different traits occurring together: a small (not medially expanded) and medially kinked head. Indeed, the ventral margin of the femoral head of *S. agudoensis* does not form a distally continuous curve, as in lagerpetids (Nesbitt *et al.* 2009b) and *Marasuchus lilloensis* (PVL 3870), but is angled relative to the shaft as in most dinosaurs (Langer & Benton 2006). The head is not medially expanded as in those forms however, matching better the condition of other basal dinosauriforms (Ezcurra 2006; Nesbitt *et al.* 2007, 2010; Irmis *et al.* 2007a; *Pseudolagosuchus major* PVL 4629).

Table 1. *Measurements (in mm) for the femora attributed to* Sacisaurus agudoensis. *Abbreviations: cc, craniocaudal; DC, compression of distal end; DW, distal width; HL, head length; HW, head width; L, left; lm, lateromedial; na, not applicable; R, right; TL, total length. Estimated measurements under brackets.*

Specimen number/side	TL	HL	HW	DW	DC	Preservation
MCN PV10009/R	87.24	13.89	6.18	9.71	lm	Entire
MCN PV10010/R	92.41	16.53	5.42	15.32	cc	Entire
MCN PV10011/R	97.32	15.99	5.96	9.47	lm	Entire
MCN PV10012/R	101.82	18.25	6.38	12.94	na	Entire
MCN PV10013/R	99.29	16.18	5.27	12.82	na	Entire
MCN PV10014/R	96.56	15.88	8.08	14.94	na	Entire
MCN PV10015/R	103.13	15.51	8.30	15.35	cc	Entire
MCN PV10016/R	(99.89)	15.86	5.77	–	–	No distal end
MCN PV10017/R	110.39	16.05	7.91	12.29	na	Entire
MCN PV10018/R	89.27	15.30	8.14	16.32	cc	Entire
MCN PV10019/R	93.14	14.63	6.30	16.66	cc	Entire
MCN PV10022/R	–	13.72	4.07	–	–	Proximal three-fifths
MCN PV10062/R	85.14	–	–	8.73	lm	No head
MCN PV10063/R	87.62	13.70	5.59	16.60	na	Entire
MCN PV10064/R	–	16.93	5.82	–	–	Proximal three-quarters
MCN PV10065/R	–	12.18	7.21	–	–	Proximal quarter
MCN PV10066/R	–	–	–	–	–	Shaft
MCN PV10067/L	–	–	–	6.1	lm	Distal half
MCN PV10068/R	–	–	–	–	–	Proximal quarter (no head)
MCN PV10069/R	–	–	–	(9.00)	–	No head (in matrix)
MCN PV10070/R	–	–	–	–	–	Proximal quarter (no head)
MCN PV10071/R	–	–	–	12.80	na	Distal quarter
MCN PV10072/R	–	–	–	13.47	na	Distal three-fifths
MCN PV10073/R	–	–	–	15.63	na	Distal fifth
MCN PV10074/R	–	–	–	13.01	na	Distal articulation
MCN PV10075/R	(97.45)	–	–	–	–	Entire (in matrix)
MCN PV10092/R	–	17.69	–	–	–	Head (in matrix)
MCN PV10098/R	–	14.51	–	–	–	Partial head
MCN PV10099/R	94.55	13.79	–	–	–	Entire (in matrix)
MCN PV10228/R	–	17.32	4.17	–	–	Proximal half
MCN PV10229/R	–	19.11	8.17	–	–	Proximal half
MCN PV10230/R	–	13.78	8.88	–	–	Proximal quarter
MCN PV10231/R	–	12.18	6.32	–	–	Proximal quarter
MCN PV10232/R	–	–	7.78	–	–	Head
MCN PV10233/R	–	–	4.08	–	–	Head
MCN PV10234/R	–	–	–	–	–	Proximal half

In some specimens, the ventral margin of the head is excavated by a broad groove ('ve' in Figs 14 & 16), surrounded by smooth bone surface both caudomedially and craniolaterally, also seen in *Silesaurus opolensis* (ZPAL AbIII/457), *Eucoelophysis baldwini* (NMMNM P-22298) and some basal dinosaurs (*Saturnalia tupiniquim*, MCP 3846-PV; Nesbitt *et al.* 2009*a*). Even if more expanded towards the caudomedial surface of the head (Fig. 16c), this seems equivalent to the 'ventral emargination' of lagerpetids (Sereno & Arcucci 1994*a*; Nesbitt *et al.* 2009*b*). Although not medially expanded, the femoral head of *Sacisaurus agudoensis* can be described as subrectangular in cranial/caudal views (Langer & Benton 2006; Langer *et al.* 2010). This is given by flattened lateral, medial and proximal margins, although the latter can be slightly convex.

Indeed, the proximal margin forms nearly straight angles to the medial and lateral margins, the latter of which corresponds to the so-called angular 'greater trochanter' of Sereno (1999). This is coupled with the proximal constraint of the femoral articular surface of silesaurids (Dzik 2003; Ezcurra 2006; Irmis *et al.* 2007*a*; Nesbitt *et al.* 2007, 2010), which does not significantly curve downwards (extending onto the medial margin of the head) as seen in other dinosauromorphs (Sereno & Arcucci 1994*b*; Ezcurra 2006; Langer & Benton 2006; Nesbit *et al.* 2009*a*, *b*). In some specimens, the femoral head has a smooth surface ('ss' in Fig. 16), which may in life have allocated a cartilaginous bursa of the hip joint.

The cranial surface of the head is marked by a strong ridge ('fcmc' in Bittencourt & Kellner
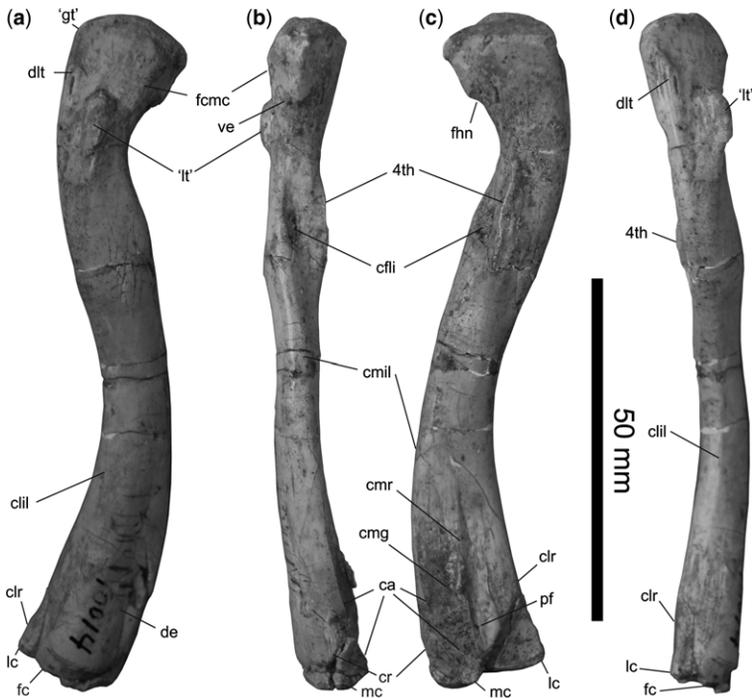
Fig. 14. *Sacisaurus agudoensis*, right femur (MCN PV10014) in **(a)** craniolateral; **(b)** craniomedial; **(c)** caudolmedial; and **(d)** caudolateral views. *Abbreviations*: 4th, fourth trochanter; ca, caudal branch of cmil; cfli, M. caudofemoralis longus insertion; clil, caudolateral intermuscular line; clr, caudolateral ridge; cmg, caudomedial groove; cmil, caudomedial intermuscular line; cmr, caudomedial ridge; cr, cranial branch of cmil; de, distal excavation; dlt, dorsolateral trochanter; fc, fibular condyle; fcmc, femoral craniomedial crest; fhn, femoral head notch; 'gt', greater trochanter; lc, lateral condyle; 'lt', lesser trochanter; mc, medial condyle; pf, popliteal fossa; ve, ventral emargination.

2009) that extends distally from the 'craniolateral tuber', separating a flat craniomedial surface ('cms' in Fig. 16) from a slightly concave area medial to the 'dorsolateral' trochanter and proximal to the 'lesser' trochanter (*sensu* Langer & Benton 2006).

The proximodistally elongated 'dorsolateral' trochanter forms the steep lateral border of that flat area, but its lateral surface is nearly continuous to the opposite side of the head. Further, it merges smoothly into the shaft distally whereas its proximal
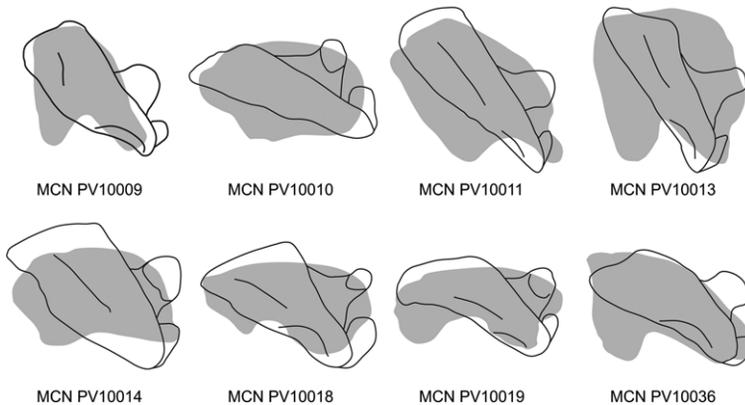
Fig. 15. *Sacisaurus agudoensis*, outlines of the proximal and distal (in grey) femoral surfaces. Not at the same scale.
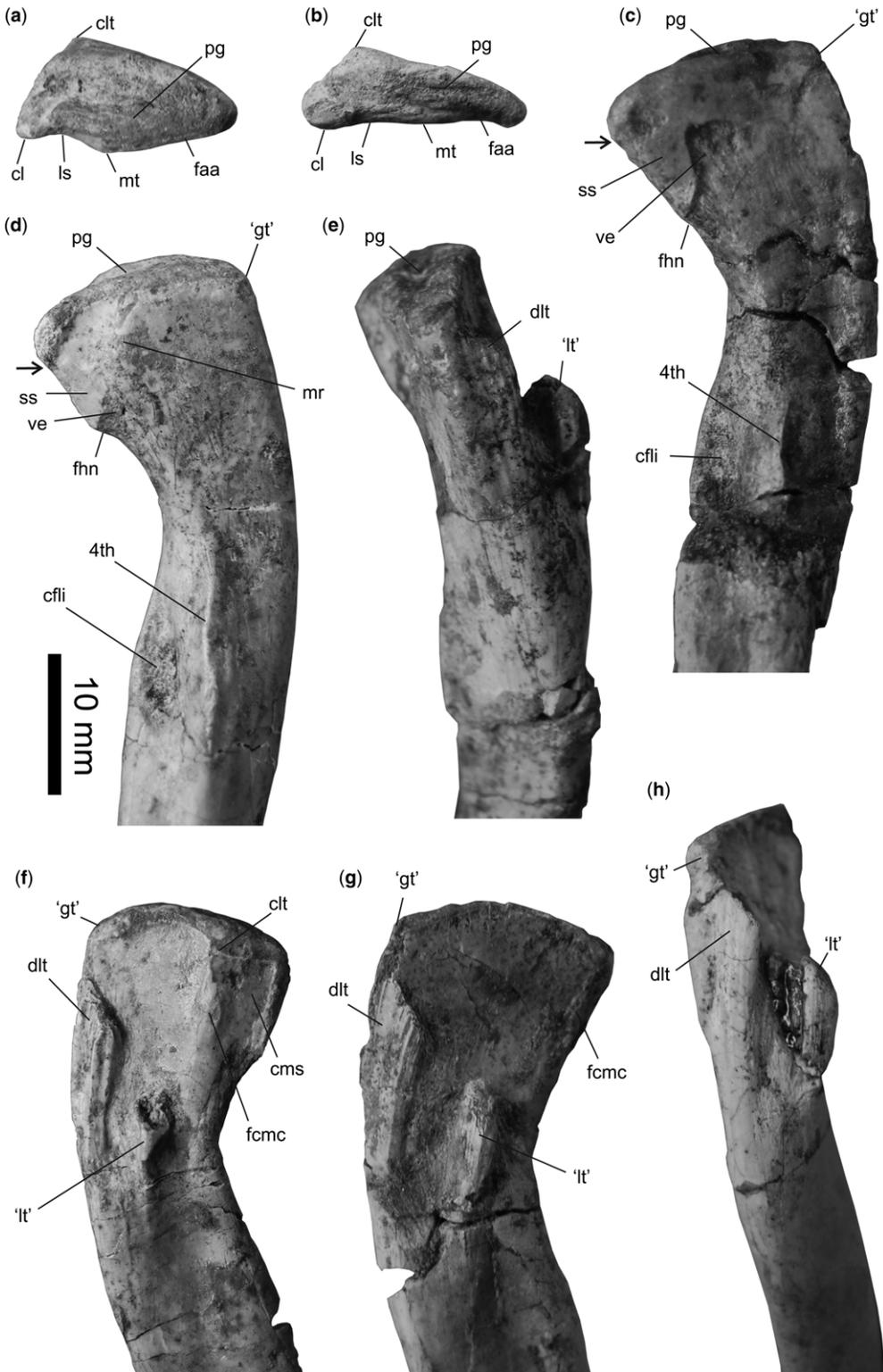
margin forms a steep angle. Its cranial and lateral surfaces bear strong longitudinal ridges and the proximal tip is crenulated, revealing muscle insertion sites. A rather similar but more proximally projected dorsolateral trochanter is seen in *Tawa hallae* (GR 241) and *Eocursor parvus* (Butler 2010), suggesting that it takes part on the 'greater trochanter' of latter ornithischians and theropods. The spike-like 'lesser' trochanter of *Sacisaurus agudoensis* is clearly projected from the femoral shaft, smooth distally, but having its proximal portion separated from the shaft by a small cleft (Fig. 16e). Despite having an ovoid cross-section, longer craniocaudally than lateromedially, it does not form a wing-like structure as seen in ornithischians (Sereno 1991; Butler 2010) and never approaches the proximal margin of the femoral head. In addition, no muscle insertion area extends laterocaudally from the 'lesser' trochanter, not forming a shelf or a 'scar leading to a bump' in the laterocaudal corner of the bone (Langer & Benton 2006). The surface between the dorsolateral and 'lesser' trochanters is however scarred for muscle insertion, which extends somewhat distally (Fig. 16g, h). More distally, cranial to the fourth trochanter, the medial surface of the femur has a marked proximodistally elongated concavity ('cfli' in Fig. 16) that probably represents the insertion of M. caudofemoralis longus. It has a sharp cranial edge and a smoother caudal margin that is nearly continuous to the extremely reduced fourth trochanter. This corresponds to a symmetrical sharp ridge with distal and proximal margins smoothly merging into the shaft. A pair of perforating foramina is present (Fig. 17a, b) cranial and proximal to the trochanter/concavity, as seen in other dinosauromorphs (Madsen 1976; Raath 1977; Madsen & Welles 2000; Carrano *et al.* 2002; Nesbitt *et al.* 2009b; Langer *et al.* 2011).

Unlike most basal dinosaurs – for example *Herrerasaurus ischigualastensis* (Novas 1993) and *Saturnalia tupiniquim* (Langer 2003) – the femoral shaft *of Sacisaurus agudoensis* lacks a conspicuous 'cranial intermuscular line' extending along its cranial surface. Instead, its caudolateral corner is marked by a longitudinal ridge (Figs 14 & 17) that may correspond to the 'caudolateral intermuscular line' of those dinosaurs. It extends distally from the area of the proximal femoral trochanters approaching the caudolateral margin of the fibular

condyle. Likewise, another ridge ('cmil' in Fig. 14) extends distally from the cranial edge of the M. caudofemoralis longus insertion along the medial surface of the femur. It flares somewhat medially about three-quarters down the shaft forming a faint flange ('cmdc' in Fig. 17g). A similar structure was described for *Dromomeron romeri* and *D. gregorii* (Nesbitt *et al.* 2009b) and also recognized in basal dinosaurs (Langer *et al.* 2011). Although less conspicuous, this may correspond to the 'craniomedial distal crest' (Hutchinson 2001) frequently hypertrophied in theropods as the 'medial epicondylar crest' (Carrano & Hutchinson 2002; Tykoski 2005; Nesbitt *et al.* 2009b). The ridge diminishes again near the distal end of the bone, where it bifurcates into caudal and cranial branches ('ca' and 'cr' in Figs 14 & 17). These reach the medial condyle and the craniomedial corner, respectively, of the distal articulation, as also seen in *Eucoelophysis baldwini* (NMMNM P-22298) and *Silesaurus opolensis* (ZPAL AbIII/361/23). Broken femora (MCN PV10070, PV10071) allow the observation of the bone wall thickness near the midshaft, which corresponds to about 0.2 of the bone diameter.

The cranial surface of the distal end of the femur is marked in its centre by a proximodistally elongated subtle excavation ('de' in Figs 14 & 17), lateral to which lies a rugose area (Fig. 17f) that possibly represents the insertion of M. femorotibialis externus (Novas 1993; Hutchinson 2001; Nesbitt *et al.* 2009b). The caudal surface of the distal end of the femur bears two pairs of proximodistally oriented grooves and ridges. The more-lateral groove is central on the bone and represents the popliteal fossa (Yates 2003), i.e. 'intercondylar groove' (Butler 2010), that extends for the whole distal third of the femur (Irmis *et al.* 2007a; Nesbitt *et al.* 2007, 2010; Nesbitt 2011). The equally long medial groove ('cmg' in Figs 14 & 17) is heavily striated, and lies right caudal to the 'caudomedial distal crest'. Between those grooves, a ridge ('cmr' in Figs 14 & 17) extends proximally from the caudal corner of the medial condyle, whereas a second ridge ('clr' in Figs 14 & 17) represents the proximal expansion of the slightly caudally kinked (MCN PV10013) lateral condyle, forming the laterocaudal corner of the distal end of the femur. Likewise, on the lateral surface of the distal end of the femur, a groove extends proximally from between

Fig. 16. *Sacisaurus agudoensis*, femoral details: **(a)** MCN PV10014 and **(b)** MCN PV10016 in proximal views; proximal portions of **(c)** MCN PV10011 and **(d)** MCN PV10014 in caudomedial view; **(e)** MCN PV10018 and **(h)** MCN PV10019 in caudolateral views; and **(f)** MCN PV10022 and **(g)** MCN PV10011 in craniolateral views. Abbreviations as in Figure 14 plus: cl, caudal lip; clt, craniolateral tuber; cms, craniomedial surface; faa, facies articularis antitrochanterica; ls, ligament sulcus; mt, medial tuber; mr, medial ridge; pg, proximal groove; ss, smooth surface. Arrow indicates distalmost extension of the articular surface of the proximal femur.
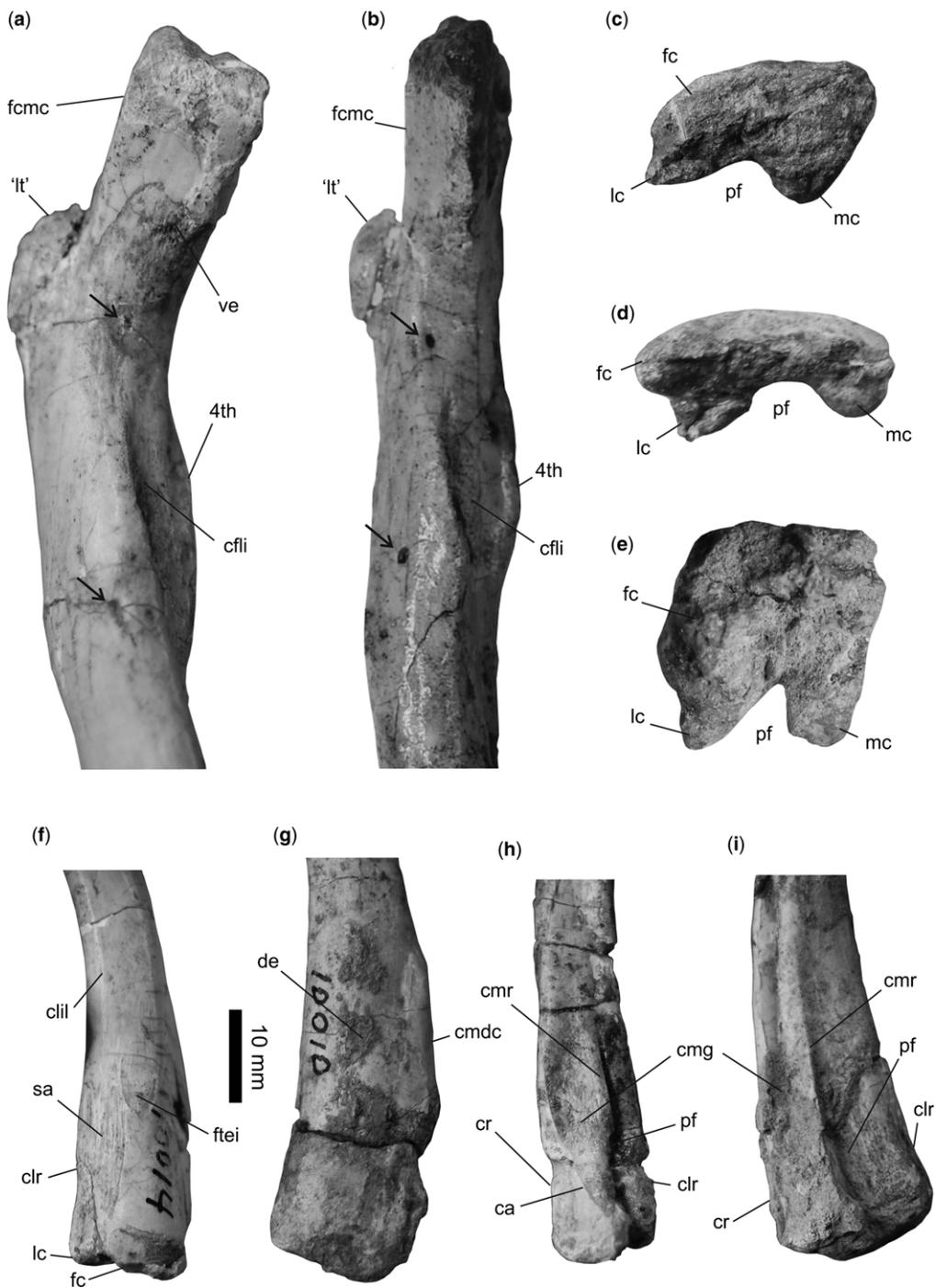
Fig. 17. *Sacisaurus agudoensis*, femoral details. Proximal portions of **(a)** MCN PV10014 and **(b)** MCN PV10013 in craniolateral views; distal view of **(c)** MCN PV10027, **(d)** MCN PV10019 and **(e)** MCN PV10013; and distal portions of **(f)** MCN PV10014 in lateral view, **(g)** MCN PV10010 in cranial view, **(h)** MCN PV10062 and **(i)** MCN PV10036 in caudomedial views. Abbreviations as in Figs 14 and 16 plus: cmdc, craniomedial distal crest; ftei, M. femorotibialis externus insertion; sa, striated area. Arrow indicates perforating foramina.

the fibular and lateral condyles, where a striated area ('sa' in Figs 14 & 17f) is seen in some specimens. The femoral distal outline varies according to the compression of the bone (Fig. 16), but it is usually broader than craniocaudally long. A groove excavates the distal surface of the bone between the fibular and medial condyles, but does not enter the craniodistal corner of the bone. In addition, a trough is seen between the former and the proximally displaced lateral condyle (MCN PV10019), which is lateromedially flattened in some specimens (MCN PV10009, PV10011) to form a crista tibiofibularis (Rowe 1989).

The Tibia & Fibula

The preserved tibiae include a left proximal fragment (MCN PV10093) and two nearly complete right bones (MCN PV10020, PV10021), 114 and 117 mm long respectively, that is, consistently longer than the femora. The bone is nearly straight with a subtriangular proximal outline (Figs 18 & 19), the medial margin of which is convex, whereas the lateral margin is markedly concave. Fibular and medial condyles are nearly aligned at the caudal margin of the proximal articulation (but the former is a bit projected caudally) and caudally separated by a narrow intercondylar notch (Butler 2010). Insertion scars for the knee extensor tendon (M. triceps femoris) and associated musculature (Dilkes 2000; Carrano & Hutchinson 2002) are seen in the cranioproximal surface of the tibia. They do not reach the proximal margin of the bone, the cranial margin of which shows only a feeble and continuous cranial expansion. Indeed, a kinked cnemial crest is not as clear as in various basal dinosauromorphs, for example *Heterodontosaurus tucki* (Santa Luca 1980), *Herrerasaurus ischigualastensis* (Novas
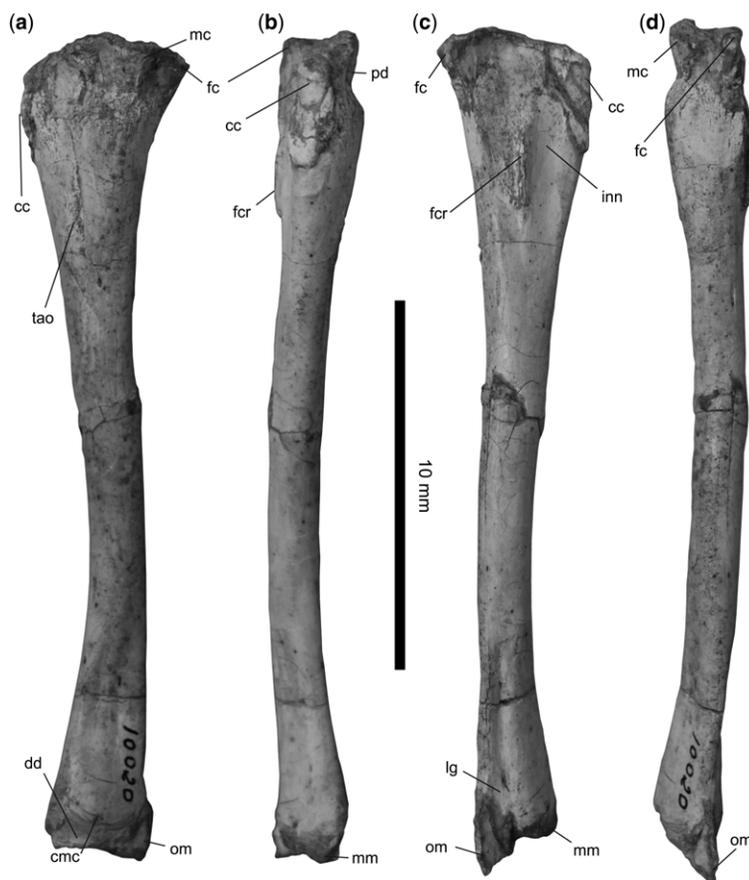
Fig. 18. *Sacisaurus agudoensis*, right tibia (MCN PV10020) in: (**a**) medial; (**b**) cranial; (**c**) lateral; and (**d**) caudal views. *Abbreviations*: cc, cnemial crest; cmc, caudomedial corner; dd, distal depression; fc, fibular condyle; fcr, fibular crest; inn, insisura tibialis; lg, lateral groove; mc, medial condyle; mm, medial malleolus; om, outer malleolus; pd, proximal depression; tao, M. Tibialis anterior origin.

1993), *Marasuchus lilloensis* (Novas 1996), *Saturnalia tupiniquim* (Langer 2003), *Dilophosaurus wetherilli* (Tykoski 2005) and *Silesaurus opolensis* (Dzik 2003), but see *Lesothosaurus diagnosticus* (Thulborn 1972), *Scutellosaurus lawleri* (Rosenbaum & Padian 2000), *Dromomeron romeri* and *D. gregorii* (Nesbitt *et al.* 2009b). The cnemial area may be defined as the entire portion of the tibia cranioproximal to the insisura tibialis (Butler 2010; lateral fossa of Carrano 2007). In lateral/medial views, its cranial apex is displaced distally from the proximal margin of the bone, as also seen in *Pisanosaurus mertii* (Irmis *et al.* 2007b). This is opposite to the typical condition among dinosaurs, the cnemial crest of which is usually proximally projected (Bittencourt & Kellner 2009; Martinez & Alcober 2009; Butler 2010). The insisura tibialis extends distally on the lateral surface of the proximal tibia, caudally bound by a well-developed fibular crest as seen in *Silesaurus opolensis* (Dzik 2003) and basal theropods (Padian 1986; Rauhut 2003), caudal to which another longitudinal groove, for the reception of the 'tibial flange' of the fibula, is seen. The most proximal portion of the medial surface of the tibia is depressed relative to the rest of the bone ('pd' in Fig. 18). Although present in the other tibiae, this depression is not seen in MCN PV10093 and probably represents a preservation artefact. A faint proximodistally elongated rugose ridge ('tao' in Fig. 18) is also seen on the medial tibia. It is bound caudally by an equally elongated depression, and possibly represents the origin of M. tibialis anterior (Carrano & Hutchinson 2002).

The tibial shaft has an ovoid cross-section at mid-length (8 mm craniocaudally and 7 mm lateromedially), but its distal third is craniolaterally to caudomedially flattened. Accordingly, the long axis of the distal tibia is oriented in the opposite direction; that is, oblique to the long axis of the proximal surface of the bone (Fig. 19c). As in the proximal margin of the bone, compression seems to have deformed the most distal portion of MCN PV10020, forming a depressed caudomedial surface ('dd' in Fig. 18). It is however possible to determine a mostly convex distal outline in that area, formed by flat to slightly concave medial and caudal surfaces separated by an obtuse corner ('cmc' in Fig. 19), but no clear ridge extends proximally from that corner. The robust craniomedial portion of the distal tibia (=medial malleolus; Butler 2010), forms a flat distal articulation that probably fitted into an equally flat surface (Novas 1996, fig. 5, 't'; Nesbitt *et al.* 2010, fig. 2 'a.ti.') on the astragalus. Its lateral portion is slightly depressed ('dtd' in Fig. 19) in relation to the medial which is nearly level with the outer malleolus, i.e. descending process (Ferigolo & Langer

2006). This depressed area probably received the astragalar ascending process, and is laterally bordered by an excavation that extends proximally along the craniolateral surface of the tibia ('lg' in Figs 18 & 19) for more than one-quarter of the total length of the bone, i.e. 'lateral groove' in Novas (1996). The caudal margin of that groove is formed by the outer malleolus, which extends as a sheet of bone caudolaterally from the main body of the distal tibia. It also expands distally, surpassing the lower extension of the medial malleolus. The outer malleolus is in fact kinked off, both distally and laterally from the average outline of the distal tibia (Fig. 19d).

Only the proximal half of the fibulae MCN PV10084 and PV10083 were recovered, the former of which is the best preserved and the basis of the following accounts. They apparently fit tibiae MCN PV10020 and PV10021, respectively, with a fair articulation in the former case, and are both inferred as bones from the right side. In lateral-medial views, the fibula expands gradually from mid-shaft towards the proximal articulation, but the expansion is more marked cranially. In proximal view, the cranial portion is also broader. The most conspicuous feature of the bone is a medial, broad and rugose 'tibial flange' extending obliquely from its cranioproximal corner. This set of features better match the left fibula of other basal dinosauromorphs, for example *Herrerasaurus ischigualastensis* (Novas 1993), *Pisanosaurus mertii* (PVL 2577), *Plateosaurus engelhardti* (GPIT 1), *Saturnalia tupiniquim* (MCP 3845-PV) and *Silesaurus opolensis* (ZPAL AbIII/361/24), rendering the side assignation of the bone somewhat ambiguous.

Metatarsals

Comparisons with *Silesaurus opolensis* (ZPAL Ab III/364) and *Saturnalia tupiniquim* (MCP 3844-PV) indicates that three of the four metatarsal elements found in the bone accumulation have relative dimensions that approximately match (difference less than 50%) the above described appendicular bones. This includes the proximal articulation of a left metatarsal II (MCN PV10239), a distal half of a right metatarsal III (MCN PV10038) and a partially prepared left metatarsal IV (MCN PV10240), the morphology of which approach those of the respective metatarsals of most basal dinosauriforms. MCN PV10238 has a trapezoidal proximal outline (Fig. 20a) with larger subparallel craniomedial and caudolateral margins and smaller caudomedial and craniolateral margins. The craniomedial surface of the bone is scarred around a smooth central area ('mla' in Fig. 20b), which probably corresponds to the articulation of metatarsal I.
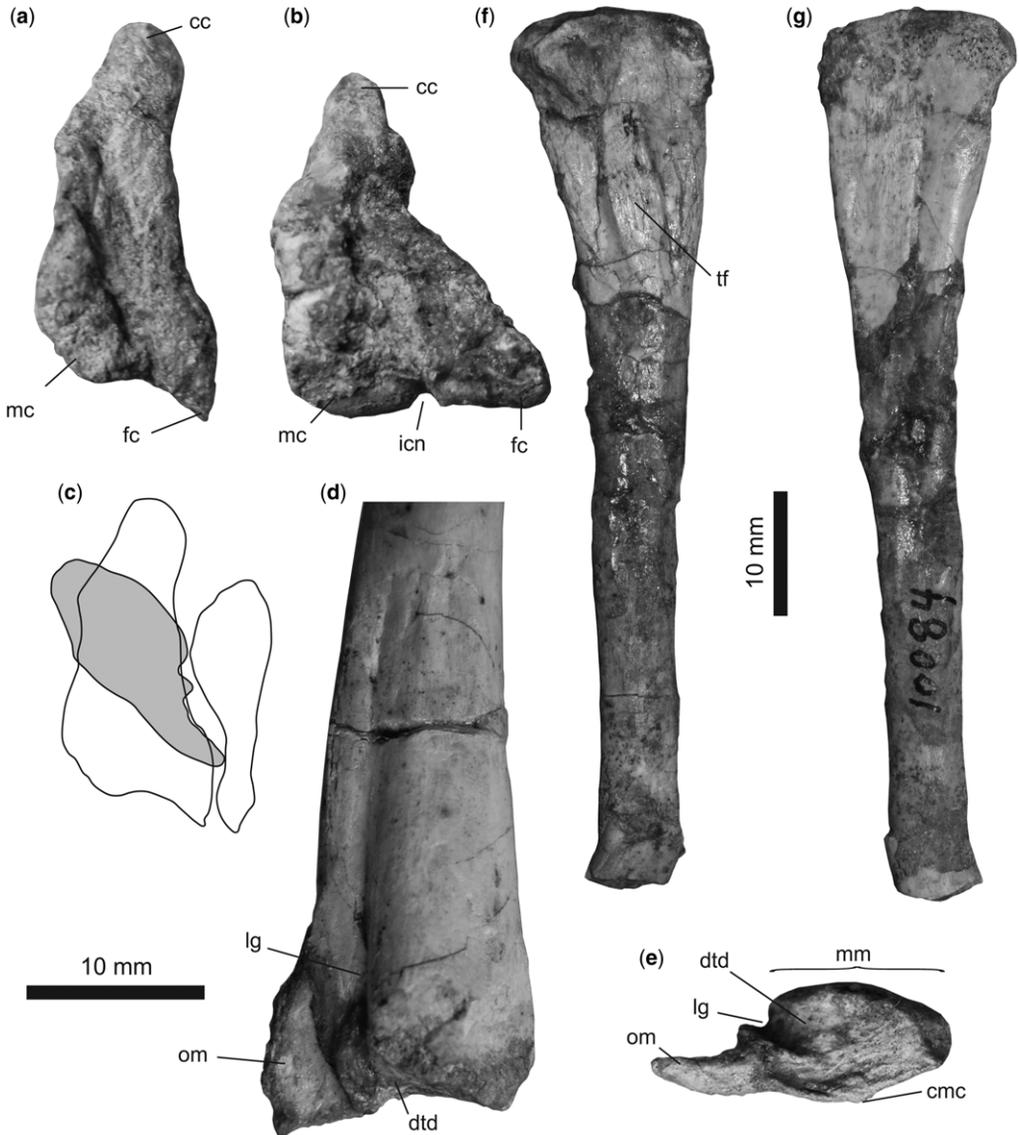
Fig. 19. *Sacisaurus agudoensis*, tibial details and fibula: **(a)** MCN PV10020 and **(b)** MCN PV10021 in proximal views; **(c)** outlines of the proximal and distal (in grey) surfaces of MCN PV10020 and proximal surface of MCN PV10084. MCN PV10020: **(d)** distal portion in craniolateral view and **(e)** distal view. MCN PV10084: **(f)** medial and **(g)** lateral views. Abbreviations as in Figure 18 plus: dtd, distal tibial depression; icn, intercondylar notch; tf, tibial flange.

The symmetrical ginglymus of MCN PV10038 (Fig. 20c–e) is broader than deep and formed of condyles of equivalent size with moderately developed collateral pits. The condyles are separated distally by a faint groove that leads to a deeper longitudinal excavation on the plantar surface. The entire distal articulation is slightly displaced medially, forming a laterally kinked margin. Its dorsal surface bears a shallow crescent-shaped extensor excavation ('ee' in Fig. 20c) with a well-marked distal rim. Available data on MCN PV10240 reveal a proximally flattened and distally tapering bone. Its exposed medial surface is proximally excavated by a broad longitudinal groove ('mg' in Fig. 20f). The distal articulation is not significantly expanded, and as deep as broad.
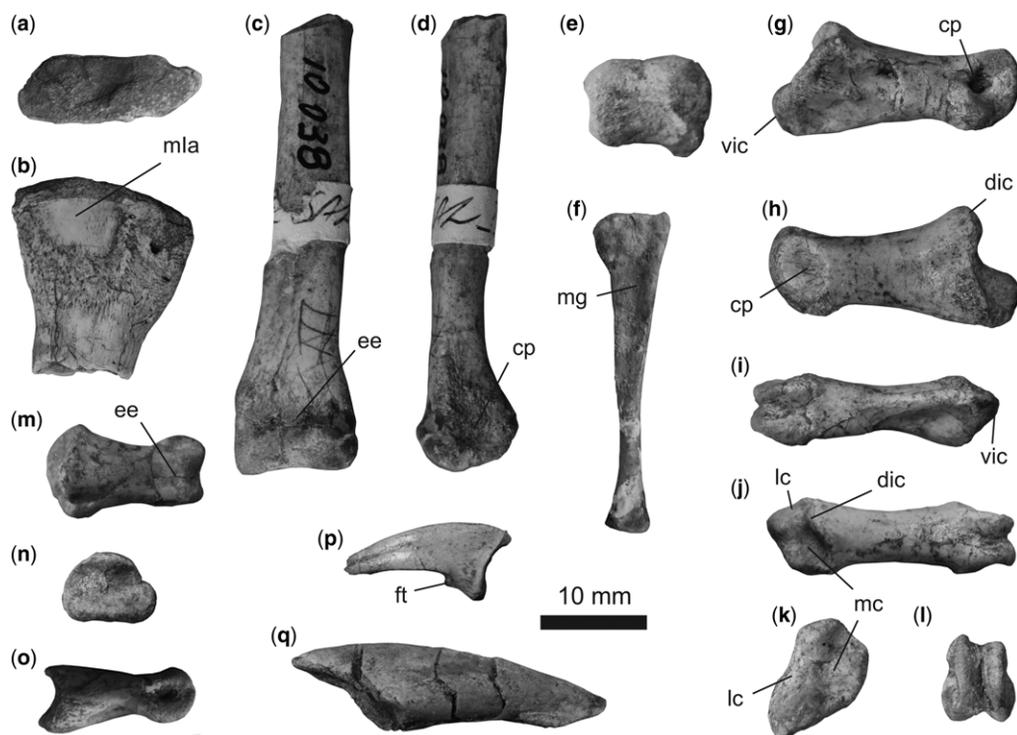
Fig. 20. *Sacisaurus agudoensis*, metatarsals and phalanges. MCN P10239 in (**a**) proximal and (**b**) medial views; MCN PV10038 in (**c**) dorsal, (**d**) medial and (**e**) distal views; (**f**) MCN PV10240 in medial view; MCN PV10039 in (**g**) medial, (**h**) lateral, (**i**) ventral, (**j**) dorsal, (**k**) proximal and (**l**) distal views; MCN PV10037 in (**m**) dorsal, (**n**) proximal, and (**o**) lateral/medial views; lateral/medial views of (**p**) MCN PV10241 and (**q**) MCN PV10242. *Abbreviations*: cp, collateral pit; dic, dorsal intercondylar process; ee, extensor excavation; ft, flexor tuber; lc, lateral cotylus; mc, medial cotylus; mg, medial groove; mla, articulation for metatarsal I; vic, ventral intercondylar process.

Phalanges

Eight isolated phalanges were found in the bone accumulation, four of which correspond to unguals. Although somewhat discrepant, the dimensions do not preclude their association with either the hand or the foot of animals of the size inferred based on the previously described skeletal remains. The larger non-ungual phalanx (MCN PV10039; Fig. 20g–l) is elongated and deeper than broad at mid-shaft. The proximal articular surface seems to be somewhat distorted by latero-medial compression, but is clearly asymmetrical. The medial cotylus is ovoid and the lateral is narrower and deeper. Both intercondylar processes are well developed, but the ventral projects further proximally. The distal ginglymus is nearly symmetrical and deeper than broad. The condyles are equally projected distally, and not significantly rotated in relation to the proximal articulation. Collateral pits are well developed, especially the medial, but no extensor pit is seen. MCN PV10037 is a stouter phalanx (Fig. 20m–o), broader than deep and not as elongated as MCN PV10039. Both proximal and distal articulations are symmetrical with equally developed proximal cotyles, intercondylar processes and distal condyles. Collateral pits are seen, as well as a faint extensor excavation. The smallest non-ungual phalanx (MCN PV10035) is more waisted than the others, but resembles MCN PV10037 in most details. Another small phalanx (MCN PV10036) preserves only the distal articulation, which is asymmetrical and deeper than broad. These are probably distal pedal phalanges, whereas MCN PV10036 and PV10039 may correspond to either a manual or a proximal pedal phalanx. The more curved preserved ungual (MCN PV10241) has a well-developed flexor tubercle ('ft' in Fig. 20p), and likely corresponds to a manual element. The other three (MCN PV10096, PV10242, PV10243) better fit the shape of pedal unguals, although those of the hand of several basal dinosauromorphs do not appear to have a much stronger curvature (Langer *et al.* 2011; Martinez *et al.*

2011). All unguals have well-developed dorsal intercondilar processes and collateral grooves for the sheath anchorage, and all have deeper than broad proximal articulations.

Phylogenetic analysis and discussion

Since its first description as a putative ornithischian dinosaur (Ferigolo & Langer 2007), *Sacisaurus agudoensis* was included in several phylogenetic studies (Brusatte *et al.* 2010; Nesbit *et al.* 2010; Benton & Walker 2011; Nesbitt 2011; Kammerer *et al.* 2012), always appearing as a member of the non-dinosaur dinosauromorph clade Silesauridae. Here, its affinity was evaluated using a modified version of the character-taxon matrix of Nesbit (2011), the most recent, comprehensive phylogenetic analysis of archosaurs to include a nearly complete sample of basal dinosauromorphs. Firstly, *S. agudoensis* was rescored (Table 2) into that matrix, based on the anatomical evidence presented here. Other modifications include the scoring of *Pseudolagosuchus major* based solely on the anatomical data available for its holotype and the exclusion of data derived from the lower jaw referred to *Lewisuchus admixtus* and the pectoral girdle and limb of *Marasuchus lilloensis*, given their uncertain association with these taxa (Arcucci 1998; Remes 2007; see Appendix I for full list of taxa and excluded characters). In addition, *Saltopus elginensis* and *Diodorus scytobrachion* were included in the data-matrix (Appendix II). The former is based on its recent revision by Benton & Walker (2011), and the latter on the codifications of Kammerer *et al.* (2012) for the character-taxon matrix of Nesbit *et al.* (2010) and the equivalence of characters between that matrix and that of Nesbitt (2011). The two characters proposed by Kammerer *et al.* (2012) were also included as characters 413 and 414 (Appendix III). Finally, various characters of Nesbit (2011) were modified regarding their definitions and, especially, scoring for taxa relevant to this study. These were chosen after an initial

analysis of the original data matrix of Nesbit (2011), when all characters that unambiguously or not supported nodes that 'fit between' the already suggested positions for *Sacisaurus agudoensis* (i.e. derived silesaurid *or* basal ornithischian) were selected for revision. Additional characters were also picked during a more arbitrary inspection performed alongside the codification of the above mentioned taxa, which were scored (Table 2; Appendix II) based on the modified versions of the characters.

The full list of modified characters is in Appendix IV, but some that deal with particularly contentious traits, as originally employed by Nesbit (2011), are highlighted in the following (these are also useful to exemplify the logics behind the performed modifications)

(1) *Jugal, posterior process: (0) lies dorsal to the anterior process of the quadratojugal; (1) lies ventral to the anterior process of the quadratojugal; (2) splits the anterior process of the quadratojugal; (3) is split by the anterior process of the quadratojugal* [character 71]. As discussed by Langer & Benton (2006), a 'forked' caudal ramus of the jugal (split by the quadratojugal) is seen in some basal ornithischians, but this condition cannot be primarily homologized (de Pinna 1991) with the bifurcated caudal portion of the jugal of heterodontosaurids (Norman *et al.* 2011; Pol *et al.* 2011), only the dorsal stem of which meets the quadratojugal. A likewise broad, caudally expanding caudal ramus of the jugal is seen in various other ornithischians (e.g. Haubold 1991) and in the best preserved partial skull of *Silesaurus opolensis* (Dzik & Sulej 2007, fig. 18a). Yet, the jugal of the latter is incomplete caudally, precluding a straightforward scoring of the character.

(2) *Supraoccipital, rugose ridge on the anterolateral edges: (0) absent; (1) present* [character 127]: *Silesaurus opolensis* (ZPAL AbIII/362/1, AbIII/364/1) and *Lewisuchus*

Table 2. *Codification for* Sacisaurus agudoensis *of the 412 characters of Nesbit (2011), as modified below (in bold), added of two (413 & 114) proposed by Kammerer et al. (2012). ? = missing data; A = 0/1, B = 1/2, C = 0/2*

??????????	**0**?**001?10**??	??**0**?000000	0?????????	??????????
??????????	????**00**????	??????????	??????????	??????????
??????????	??????????	??????????	?????**121**??	??????????
01**00**1????**0**	0????10201	1110??1???	??????????	???**?1**?????
??????????	1?????1101	?????**?1?**?**0**	00?**1001**???	**0**?????????
??????????	???021?**1**?0	10**A????**00	0????1?**0**?0	10**B**?**00**??11
C011101**211**	00**A**1110101	01**B**110**A**100	10**12110100**	**1**?????????
??????????	??????????	??????????	??????????	**11**??????**0**
??????????	??**11**			

(a) 127-1
(b) 127-1
(c) 127-1
(d) 127-1
(e) P-50529 152-1
(f) 152-1
(g) 233-1
(h) 233-1
(i) 233-1
(j) 304-0
(k) 304-1
(l) 304-2
(m) 304-2
(n) 308-2
(o) 308-3
(p) 308-2
(q) 308-1
(r) 334-1
(s) 334-2
(t) 334-2
(u) 334-2
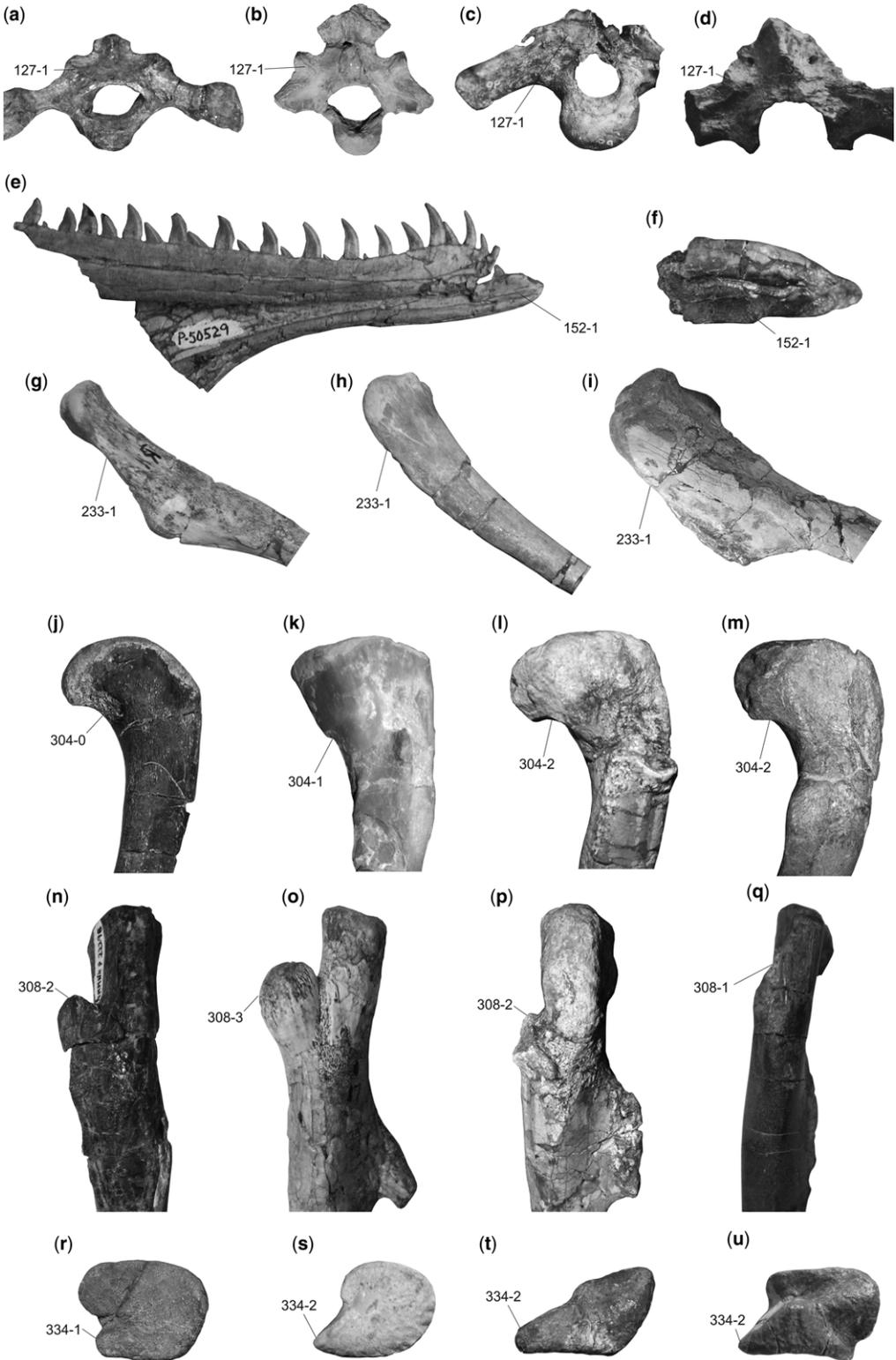
admixtus (UNLR 01) possess a rugose ridge that extends craniolaterally from the dorsolateral corner of the foramen magnum, along the exoccipital-opistotic/supraoccipital contact, separating two recesses at the dorsolateral edge of the braincase (Fig. 21a, b). This was considered a Silesauridae synapomorphy, but a similar ridge is seen in other basal dinosauromorphs/dinosaurs, for example *Marasuchus lilloensis* (PVL 3872), *Eocursor parvus* (Butler 2010), *Scelidosaurus harrisonii* (Fig. 21c) and *Plateosaurus engelhardti* (Fig. 21d). Indeed, this ridge separates the remainder of the postemporal fenestra (Sampson & Witmer 2007, *non* Norman *et al.* 2011) laterally, from a depression (frequently opened) in the supraoccipital medially. Both apertures tend to close along dinosaur evolution, but foramens are left (frequently internalized in the braincase bones) as vascular pathways (Langer & Benton 2006).

(3) *Anterior half of the dentary, position of the Meckelian groove: (0) dorsoventral centre of the dentary; (1) restricted to the ventral border* [character 152]*: contra* Nesbitt (2011) the rostral part of the Meckelian groove is located on the ventral portion of the dentary in most basal dinosauriforms/dinosaurs, for example *Coelophysis bauri* (Fig. 21e), *Dilophosaurus wetherilli* (UCMP 37303) and *Tawa hallae* (GR 241). In *Asilisaurus kongwe*, this corresponds to the elongated concavity (Fig. 21f) ventral to 'Mg' and caudal to 'f' in Nesbitt *et al.* (2010; fig. 1).

(4) *Dentary, anterior extremity: (0) rounded; (1) tapers to a sharp point* [character 155] & *Dentary teeth: (0) present along entire length of the dentary; (1) absent in the anterior portion; (2) completely absent* [character 166]. It is clear that the ornithischian predentary has several differences relative to the toothless tip of the 'silesaurid' lower jaw (the first one being the explicit individualization from the rest of the mandible), and this was scored

accordingly in Character 151 of Nesbitt (2011). There is, however, no evidence to homologize the edentulous mandible tip of 'silesaurids' to the toothed rostral portion of the ornithischian dentary, let alone to suggest that the embryological forerunners of the predentary bone are not present in the jaws of other tetrapods. Accordingly, it is at least equally likely that the toothless jaw tips of both groups are equivalent, given that both competing hypotheses require (inexistent) positive homology statements. Moreover, even if 'neomorphic', the predentary is most probably a modification of the rostral portion of the lower jaw; otherwise, from which anatomical part it is derived? In fact, almost any reputed anatomical novelty is preceded by a more or less easily identified structure (Müller & Wagner 1991; Moczek 2008). Accordingly, we prefer to take a strictly topographic approach (Remane 1952; Wiley 1975; Rieppel & Kearney 2002) and use 'lower jaw' instead of 'dentary' (see Appendix IV). As an aside, *contra* Nesbitt (2011, p. 241) the absence of a toothless mandible tip in the putative silesaurid *Lewisuchus admixtus* is no strong evidence that this condition was acquired convergently in Silesauridae and Ornithischia, because both the affinities of *L. admixtus* and the referral of its lower jaw remain highly controversial.

(5) *Humerus, proximal articular surface: (0) continuous with the deltopectoral crest; (1) separated by a gap from the deltopectoral crest* [Character 233]*: the expanded deltopectoral crest of dinosaurs is connected to the proximal articulation of the humerus by a ridge, as in *Liliensternus liliensterni* (HMN MB.R. 2175), *Saturnalia tupiniquim* (MCP 3844-PV) and *Scutellosaurus lawleri* (MNA 175). The same ridge is seen in *Silesaurus opolensis* (ZPAL AbIII 411/11, 452), but it is much harder to identify because the crest is not expanded, giving the impression that

Fig. 21. Some discussed anatomical traits. Occipital view of the braincase in (**a**) *Lewisuchus admixtus*, UNLR 01; (**b**) *Silesaurus opolensis*, ZPAL AbIII/364/1; (**c**) *Scelidosaurus harrisonii*, NHMUK R1111; and (**d**) *Plateosaurus engelhardti*, HMN A58. (**e**) Partial lower jaw pair of *Coelophysis bauri*, NMMNM P-50529. (**f**) Rostral tip of the left lower jaw of *Asilisaurus kongwe*, NMT RB9, in medial view. Lateral view of the proximal part of the humerus in (**g**) *Scutellosaurus lawleri*, MNA 175 (right side, reversed); (**h**) *Silesaurus opolensis*, ZPAL AbIII/452 (left side); and (**i**) *Dilophosaurus wetherilli*, UCMP 37302 (left side). Proximal part of the left femur: craniolateral view in (**j**) *Dromomeron romeri*, GR 218; (**k**) *Silesaurus opolensis*, ZPAL AbIII/457; (**l**) *Saturnalia tupiniquim* MCP 3844-PV; and (**m**) *Herrerasaurus ischigualastensis*, PVSJ 373; Caudolateral view in (**n**) *Eucoelophysis baldwini*, NMMNM P-22298; (**o**) *Scutellosaurus lawleri*, MNA 175; (**p**) *Saturnalia tupiniquim* MCP 3844-PV; and (**q**) *Tawa hallae*, GR 421. Distal view of the tibia in (**r**) *Herrerasaurus ischigualastensis*, PVL 2558 (left side, reversed); (**s**) *Silesaurus opolensis*, ZPAL AbIII/415/2 (right side); (**t**) *Eocursor parvus*, SAM-PK-K8025 (right side); and (**u**) *Dilophosaurus wetherilli*, UCMP 77270 (right side). Images not at the same scale. Numbers in the figures indicate characters from Nesbitt (2011) followed by character states as scored here.

the crest is continuous to the articular surface (Fig. 21g–i). The humerus of *Lewisuchus admixtus* (UNLR 01) is broken in the latero-proximal corner, meaning that the state is not possible to determine.

(6) *Femur, ventral to the proximal head: (0) smooth transition from the femoral shaft to the head; (1) notch; (2) concave emargination* [character 304]: a 'notch' ventral to the femoral head is indeed typical of silesaurids (Irmis *et al.* 2007a; Nesbitt *et al.* 2010), but this is interpreted here as the conjunction of at least two different character states, that is, a small (not craniomedially expanded) head that lacks a smooth transition to the femoral shaft, different combinations of which are seen among basal dinosauromorphs. The femoral head of lagerpetids is craniomedially projected (Fig. 21j), but follows smoothly onto the shaft (Nesbitt *et al.* 2009b). On the contrary, most dinosaurs have the head/shaft transition marked by an angle (Ezcurra 2006; Langer & Benton 2006; 'concave emargination' of Nesbitt 2011), which is simply an enlarged version of the silesaurid 'notch' because the head is medially projected (Fig. 21l–m). We redefined the character (Appendix IV) to emphasize the presence of a kinked head (seen in 'silesaurids' and dinosaurs), creating a subsidiary state for dinosaurs in which that condition is coupled with an expanded head.

(7) *Femur, anterior trochanter (=M. iliofemoralis cranialis insertion): (0) absent; (1) present and forms a steep margin with the shaft, but is completely connected to the shaft; (2) present and forms a steep margin with the shaft and separated from the shaft by a marked cleft* [character 308]. In various basal dinosaurs/dinosauromorphs the M. iliofemoralis cranialis insertion in the femur forms a 'knob-like' structure (Fig. 21n, p) that slightly protrudes proximally (with its proximal tip separated from the shaft by a cleft); this condition is intermediate between the above states 1–2 and was added here (Appendix IV).

(8) *Tibia, posterolateral flange of the distal portion: (0) absent; (1) present and contacts fibula; (2) present and extends well posterior to the fibula* [character 334]. As stressed by Nesbit (2011), the outer malleolus of *Silesaurus opolensis* not only reaches the fibula, but it is much more laterally projected (Fig. 21s) than that of many basal dinosaurs; for example compare Dzik (2003; fig. 13b) with Langer & Benton (2006; fig. 13). The character was redefined in order to represent

that morphological diversity (Appendix IV). It is also easier to score because it does not require articulated fibula or tarsals.

The modified data-matrix was analysed with *TNT v. 1.1* (Goloboff *et al.* 2008) under the same parameters employed by Nesbitt (2011), but with *Lewisuchus admixtus* and *Pseudolagosuchus major* as different taxa and characters 304, 308 and 334 as additive. The analysis resulted in 2630 MPTs (Most Parsimonious Trees) of 1327 steps, the strict consensus of which differs from that recovered by Nesbitt (2011) on the relationships of basal dinosauriforms (Fig. 22). Fewer taxa unambiguously belong to Silesauridae (including only *Diodorus scytobrachion*, *Sacisaurus agudoensis* and the type genus), which forms a polytomic clade along with *Eucoelophysis baldwini*, *Pisanosaurus mertii* and other ornithischians. Other basal dinosauriforms, that is, *Saltopus elginensis*, *Asilisaurus kongwe*, *L. admixtus* and *P. major*, fall within a larger polytomy that also includes the ornithischian and saurischian branches. This lack of resolution may be partly due to both the inclusion of incomplete/poorly constrained taxa such as *S. elginensis* (equally or more incomplete, but better constrained taxa such as *D. scytobrachion* are less problematic) and the more strict approach taken on specimen referral to terminal taxa (particularly in the case of *P. major*). The position of that latter taxon would probably be more stable if specimens other than its incomplete holotype were included in the analysis. Yet, we believe that reliability has priority over resolution in phylogenetic studies, and prefer to only broaden the circumscription of terminal taxa based on comprehensive alpha-taxonomic reviews (which are lacking in this case). Besides, as was the case in the first run of the analysis of Nesbit (2011, p. 242), the separate inclusion of *L. admixtus* and *P. major* probably reduced the topology resolution. The unresolved (sauropodomorph, herrerasaur) or unpredicted (ornithischian) phylogenetic organization within dinosaur subgroups is not the focus of this reanalysis and will not be discussed further. They may result from restricted character sampling, and the topology could easily be more structured with the inclusion of additional characters (Langer & Benton 2006; Butler *et al.* 2008; Novas *et al.* 2011) that change along those branches.

The background structure of the data agrees with some previously proposed hypotheses of relationship not depicted in the strict consensus tree, indicating directions to be explored in future research. Bootstrap resampling hints that *Pisanosaurus mertii* is probably nested with other traditional ornithischians, whereas *Eucoelophysis baldwini* groups with 'core-Silesauridae'. Surely the high

Fig. 22. Excerpt of the 'strict consensus tree' recovered from the analysis of a modified version of the character-taxon matrix of Nesbitt (2011), depicting the interrelationships of basal dinosauromorphs. Bootstrap and 'Bremer support' values for each clade are indicated in the ellipses. Black ellipses indicate better supported nodes (Bootstrap value above 50%); white ellipses indicate less supported nodes. Shown statistics (CI, consistency index; HI, homoplasy index; RI, retention Index; RCI, rescaled consistency index) correspond to the entire tree.

levels of missing entries, added of some ambiguous phylogenetic signal, seem responsible for the lack of resolution in the positions of those two taxa. Regarding the terminal taxa of the more basal polytomy, alternate inclusion of only *Asilisaurus kongwe* and *Pseudolagosuchus major* results in their placement as the sister taxon to the Ornithischia/Silesauridae clade. This suggests that both taxa bear traits supporting their nesting within that group, but these are not the same and their phylogenetic signal are weakened if *A. kongwe* and *P. major* are included together in the analysis. Therefore, it is not only the abundance of missing entries, but more probably the ambiguity of phylogenetic signals that is lowering resolution in that part of the tree. On the contrary, the exclusion of only *Satopus elginensis* enforces an odd placement of *Lewisuchus admixtus* into the saurischian lineage.

The ornithischian affinity of silesaurids was inferred by Ferigolo & Langer (2007) and Niedzwiedzki *et al.* (2009), but never backed up by a numerical study. The present analysis partially fills that gap, but it is not suggested that it represents a robust hypothesis of relationship. Indeed, bootstrap and 'Bremer support' values show that all recovered

clades on the Ornithischia + Silesauridae branch are weakly supported (Fig. 22), and suboptimal trees excluding all putative silesaurids from Dinosauria are only a single step longer than the MPTs. Also, there are only a few characters that optimize (ambiguously or unambiguously) as synapomorphic for the members of that clade, namely: enlarged and coarser tooth serrations (=denticles); 'insertion' of vertebrae between first and second primordial sacral vertebrae; scapular blade longer than 3 times its dorsal width; 'lesser trochanter' separated from the femoral shaft by a cleft; femur lacking a 'trochanteric shelf' (reversion); femur with facies articularis antitrochanterica level with the 'greater trochanter' (reversion); fibular condyle at the caudal margin of the proximal tibia; outer malleolus extending well lateral to the craniolateral corner of the distal tibia; and no astragalar caudal groove. In fact, the most significant outcome of this reanalysis is the understanding that uncertainties still pervade the phylogeny of basal dinosaurs-dinosauriforms. Most characters that support nodes in that part of the phylogeny are prone to reinterpretations, which can result in radically different hypotheses of relationship. This is also the case of those uniting

Sacisaurus agudoensis and *Diodorus scytobrachion* (Kammerer *et al.* 2012). A significant decrease in tooth size in the rostral portion of the dentary is also seen in a number of ornithischians (Thulborn 1974; Galton 1978; Norman *et al.* 2007), whereas more rostral teeth of *Silesaurus opolensis* (Dzik & Sulej 2007, fig. 18a) are as rostrally canted as those of *Sacisaurus agudoensis*.

Regardless of its poor support, the outcome of this phylogenetic study is so novel that minor comments are mandatory. Most studies understand the rise of dinosaurs as a relatively rapid burst of diversity and anatomical change during the Late Triassic, coupled with the initial cladogenic events of the saurischian and ornithischian lineages (Brusatte *et al.* 2010; Langer *et al.* 2010; Irmis 2011). In contrast, the possible nesting of Middle Triassic silesaurids into the Ornithischia branch suggests a long fuse model for dinosaur radiation, with its basal (Ornithischia–Saurischia) split occurring during the late, perhaps even early, Middle Triassic, but their rise in diversity/disparity postponed until the later in that Period. Clearly, additional data are required to fully test this hypothesis.

Appendix I

Characters of Nesbitt (2011, as modified in Appendix IV) codified as '?' for the given taxa (explanation provided in brackets):

Marasuchus lilloensis (scored from the pectoral girdle and limb of PVL 3871 probably not referable to the taxon; Remes 2007): 212, 216–217, 219, 224, 227, 230–232, 234–237 and 241.

Lewisuchus admixtus (scored from the lower jaw of UNLR 1 uncertainly attributed to the taxon): 151–155 and 166.

Pseudolagosuchus major (not possible to score based on PVL 4629): 200–209, 264–265, 270, 272–277, 287, 297, 307, 314, 325, 333, 340, 358, 360, 366, 372–376, 378–381 and 401.

Appendix II

Characters of Nesbitt (2011, as modified in Appendix IV) scored for additional taxa:

Diodorous scytobrachion – based on Kammerer *et al.* (2012; original codifications of those authors under brackets):152 = 1;153 = 0;167 = 0;168 = 2;169 = 0; 171 = 1; 172 = 0; 173 = 1; 174 = 0; 230 = 0; 232 = 0; 233 = ? (0); 234 = 1; 235 = 0; 300 = 1; 301 = 0 (2); 302 = 0 (1); 303 = 1; 304 = 1; 306 = 0; 307 = 1; 308 = 1/2 (0); 309 = 1; 310 = 0; 311 = 0 (?); 313 = 0; 314 = 1 (0); 316 = 1; 317 = 0; 319 = 0; 320 = 1; 322 = 0; 324 = 1; 325 = 0; 326 = 0; 327 = 0, 413 = 1, 414 = 1.

Saltopus elginensis (based on NHMUK R3815 and Benton & Walker 2011): 205 = 0; 206 = 0; 207 = 0; 212 = 1; 216 = 0; 217 = 1; 218 = 0; 230 = 0; 231 = 0; 232 = 0; 233 = 1; 235 = 0; 236 = 0; 241 = 1; 242 = 0; 243 = 0; 245 = 1; 253 = 0; 256 = 1; 258 = 0; 259 = 0; 260 = 0; 268 = 1; 269 = 0; 270 = 0; 275 = 0; 278 = 1; 279 = 0; 282 = 0; 283 = 0; 294 = 1; 295 = 0; 296 = 0; 299 = 1; 308 = 1; 311 = 1; 358 = 0; 365 = 1; 367 = 0; 370 = 0; 373 = 0; 374 = 0; 382 = 1; 383 = 1; 384 = 1; 388 = 0; 390 = 0; 393 = 1; 395 = 1; 396 = 0; 399 = 2; 400 = 0.

Appendix III

Codification of the two characters added by Kammerer *et al.* (2012) to taxa present in the data-matrix of Nesbitt (2011).

Mesosuchus (00), *Prolacerta* (00), *Archosaurus* (00), *Proterosuchus* (00), *Erythrosuchus* (00), *Vancleavea* (00), *Chanaresuchus* (00), *Tropidosuchus* (00), *Euparkeria* (00), *Parasuchus* (00), *Smilosuchus* (00), *Pseudopalatus* (00), *Gracilisuchus* (00), *Turfanosuchus* (00), *Ornithosuchus* (00), *Riojasuchus* (00), *Revueltosaurus* (00), *Stagonolepis* (00), *Aetosaurus* (00), *Longosuchus* (00), *Ticinosuchus* (00), *Qianosuchus* (00), *Xilousuchus* (00), *Arizonasaurus* (?0), *Poposaurus* holotype (??), *Poposaurus* Yale (??), *Lotosaurus* (??), *Sillosuchus* (??), *Effigia* (??), *Shuvosaurus* (??), *Prestosuchus* (00), UFRGS 1565 T (00), UFRGS 01525 T (00), Combined *Prestosuchus* (00), *Saurosuchus* (00), *Batrachotomus* (00), *Postosuchus kirkpatricki* (00), *Dromicosuchus* (??), *Fasolasuchus* (00), *Rauisuchus* (??), *Polonosuchus* (00), *Postosuchus alisonae* (00), CM 73372 (00), *Hesperosuchus agilis* (00), *Hesperosuchus* ''*agilis*'' (00), *Dibothrosuchus* (0?), *Terrestrisuchus* (00), *Sphenosuchus* (00), *Litargosuchus* (??), *Kayentasuchus* (00), *Orthosuchus* (00), *Alligator* (00), *Protosuchus haughtoni* (00), *Protosuchus richardsoni* (00), *Eudimorphodon* (00), *Dimorphodon* (00), *Lagerpeton* (??), *Dromomeron gregorii* (??), *Dromomeron romeri*

(??), *Marasuchus* (??), *Asilisaurus* (??); *Silesaurus* (00), *Eucoelophysis* (??), *Lewisuchus* (??), *Pseudolagosuchus* (??), *Pisanosaurus* (00), *Lesothosaurus* (10), *Heterodontosaurus* (00), *Eocursor* (??), *Scutellosaurus* (1?), *Herrerasaurus* (00), *Staurikosaurus* (0?), *Eoraptor* (??), *Saturnalia* (0?), *Plateosaurus* (00), *Efraasia* (00), *Tawa* (00), *Coelophysis* (00), *Dilophosaurus* (00), *Allosaurus* (00), *Velociraptor* (00).

Appendix IV

Characters revised from Nesbitt (2011): 6, 9, 44, 56, 67, 71, 75, 95, 110, 113, 115, 127, 141, 144, 152, 153, 154, 155, 158, 166, 168, 171, 172, 173, 174, 181, 183, 186, 195, 207, 208, 212, 214, 218, 222, 230, 233, 241, 258, 271, 273, 274, 289, 294, 297, 299, 301, 303, 304, 308, 309, 310, 311, 313, 314, 316, 317, 323, 324, 325, 328, 331, 333, 334, 335, 336, 362, 363, 366, 373, 378, 400.

Obs. I. characters listed above but not discussed below were revised, but not modified, and their definition/scoring follow that of Nesbitt (2011).

Obs. II: underlined characters above were arbitrarily selected during the recodification of taxa, and do not represent apomorphies of 'intermediary' clades (see text for discussion).

6 – **Scoring**: *Scutellosaurus* = 3 (MNA 175).

9 – **Scoring**: *Scutellosaurus* = 0 (MNA 175).

67 – **Scoring**: *Lewisuchus* = 0 (UNLR 1).

Obs.: *Lewisuchus* has an extensive dorsal ramus of the jugal that fits caudomedial to the postorbital, as also seen in some basal dinosaurs (*Eoraptor*, PVSJ 512; *Lesothosaurus*, NHMUK RUB23, Knoll 2002).

71 – **Scoring**: *Heterodontosaurus* = ?(Norman *et al.* 2011); *Silesaurus* = (Dzik & Sulej 2007; Fig. 18a).

75 – **Scoring**: *Lewisuchus* = 1 (UNLR 1); *Heterodontosaurus* = ? (Norman *et al.* 2011); *Silesaurus* = 1 (Dzik & Sulej 2007; Fig. 18a).

Obs.: the jugal ornamentation of *Heterodontosaurus* does not fit any of the proposed states of this character; the jugal crest of *Silesaurus* and *Lewisuchus* resemble that of *Herrerasaurus* and *Eoraptor* (respectively), which were scored as '1'.

110 – **Scoring**: *Eoraptor* = ?(PVSJ 512); *Heterodontosaurus* = 1? (Norman *et al.* 2011); *Marasuchus* = ? (PVL 3872).

113 – **Scoring**: *Marasuchus* = ?(PVL 3872).

115 – **Scoring**: *Heterodontosaurus* = ?(Norman *et al.* 2011); *Lewisuchus* = ?(UNLR 01); *Marasuchus* = ? (PVL 3862); *Silesaurus* = ?(ZPAL various specimens).

Obs.: the exoccipital-basioccipital suture is not clear in any basal dinosauromorph, especially inside the braincase, and this character cannot be estimated with confidence; in *Silesaurus*, ZPAL Ab III/361/35 inconclusively suggests state 1.

127 – **Scoring**: *Eocursor* = 1 (Butler, 2010); *Marasuchus* = 1 (PVL 3872); *Plateosaurus* = 1 (HMN A58).

152 – **Scoring**: *Asilisaurus* = 1 (NMT RB9); *Coelophysis* = 1 (NMMNM P-50529); *Dilophosaurus* = 1 (UCMP 37303); *Eoraptor* = ?(PVSJ 512); *Staurikosaurus* = ?(MCZ 1669); *Tawa* = 1 (GR 241).

153 – **Scoring**: *Silesaurus* = 0 (ZPAL AbIII/437/1).

154 – **Scoring**: *Heterodontosaurus* = 0 (Norman *et al.* 2011); *Scutellosaurus* = 0 (MNA 175).

155 – **Definition**: Lower jaw, rostral extremity: rounded (0); tapers to a sharp point (1).
Scoring: *Heterodontosaurus* = 1 (Norman *et al.* 2011); *Lesothosaurus* = 1 (Sereno, 1991); *Pisanosaurus* = ? (PVL 2577); *Scutellosaurus* = ?(MNA 175).

158 – **Scoring**: *Asilisaurus* = ?(NMT RB140).

166 – **Definition**: Lower jaw teeth: present along entire length of the jaw (0); absent in the rostral portion (1); completely absent (2).
Scoring: *Eocursor* = ?(Butler 2010); *Heterodontosaurus* = 1 (Norman *et al.* 2011); *Lesothosaurus* = 1 (Sereno, 1991); *Pisanosaurus* = ?(PVL 2577).

168 – **Scoring**: *Silesaurus* = 1/2 (ZPAL Ab III 404/1).

Obs.: tooth serrations in *Sacisaurus* and ornithischians are coarser than in *Silesaurus*, but the latter taxon also has relatively large denticles oblique to the tooth margin, especially in more caudal teeth.

172 – **Scoring**: *Heterodontosaurus* = 0 (Norman *et al.* 2011); *Lesothosaurus* = 1 (Sereno 1991); *Scutellosaurus* = 1 (MNA 175); *Silesaurus* = 1 (ZPAL Ab III/437/1).

Obs.: a cingulum, i.e. an asymmetric (more developed on the lingual side) basal swelling of the crown, was considered present in all ornithischians included in the data-matrix, except for *Heterodontosaurus* (Butler *et al.* 2008; Butler 2010); this is also the case of *Silesaurus*, as clearly seen in teeth number 2, 4 and 5 of the holotype.

174 – **Scoring**: *Lewisuchus* = 1 (UNLR 01).

Obs.: there is as much evidence for *Lewisuchus* as there is for most basal dinosaurs that their teeth are not fused to the bone of attachment.

181 – **Scoring**: *Asilisaurus* = ?(articulated column unavailable); *Lesothosaurus* = ?(articulated column unavailable); *Plateosaurus* = 1 (GPIT 1).

183 – **Scoring**: *Asilisaurus* = ?(articulated vertebrae unavailable).

212 – **Scoring**: *Heterodontosaurus* = 0 (Santa Luca, 1980).

218 – **Scoring**: *Coelophysis* = 0 (AMNH 7224); *Herrerasaurus* = 1 (PVSJ 53); *Lesothosaurus* = 0 (NHMUK RUB17); *Lewisuchus* = 0 (UNLR 1).

222 – **Scoring**: *Coelophysis* = 1 (NMMNHS 42577); *Efraasia* = 1 (SMNS 12667, 12843); *Eoraptor* = 1 (PVSJ 512); *Herrerasaurus* = 1 (Brinkman & Sues 1987); *Plateosaurus* = 1 (GPIT 1); *Saturnalia* = 1 (Langer *et al.* 2007).

230 – **Scoring**: *Asilisaurus* =?(complete humerus unavailable); *Lesothosaurus* = 0 (NHMUK RUB17).

233 – **Scoring**: *Dilophosaurus* = 1 (UCMP 37302); *Lewisuchus* = ?(UNLR 1); *Saturnalia* = 1 (MCP 3844-PV); *Silesaurus* = 1 (ZPAL AbIII 411/11, 452);

271 – **Scoring**: *Asilisaurus* = ?(NMT RB13); *Efraasia* = 1 (SMNS 12354); *Plateosaurus* = 1 (GPIT 1).

273 – **Scoring**: *Asilisaurus* = 0 (NMT RB13); *Eucoelophysis* = ?(NMMNM P-22298); *Scutelosaurus* = (MNA 175).

274 – **Scoring**: *Asilisaurus* = 1 (NMT RB13); *Eucoelophysis* = ?(NMMNM P-22298); *Silesaurus* = 1 (ZPAL Ab III 404/1).

Obs.: the acetabular antitrochanter is indeed not well marked in 'silesaurids' but not less than in *Marasuchus* and most basal dinosaurs.

289 – **Scoring**: *Marasuchus* = 1 (PVL 3870).

Obs.: the distal pubic margin of *Marasuchus* is not much narrower than the proximal width of the bone but equivalent to that seen in *Pseudolagosuchus*, which was scored as '1'; here we are not employing the codification as suggested by Langer & Benton (2006, fig. 10).

297 – **Scoring**: *Asilisaurus* = ?(NMT RB12); *Efraasia* = 1 (SMNS 12354); *Herrerasaurus* = 1 (PVL 2566); *Pisanosaurus* = ?(PVL 2577); *Plateosaurus* = 1/2 (various specimens); *Saturnalia* = 1 (MCP 3844-PV); *Scutellosaurus* = 1 (UCMP 130580).

301 – **Scoring**: *Eucoelophysis* = 0 (NMMNM P-22298); *Lesothosaurus* = 2 (NHMUK RUB17); *Silesaurus* = 0/2 (ZPAL AbIII 1272, 361/23, 457).

304 – **Definition**: Femur: smooth transition from the femoral shaft to the head (0); kinked transition from the femoral shaft to the head (1); kinked transition and expanded head (2). **ORDERED**

308 – **Definition**: Femur, anterior trochanter (= M. iliofemoralis cranialis insertion): (0) absent; (1) present and forms a steep margin with the shaft, but is completely connected to the shaft; (2) present and separated from the shaft by a cleft; (3) present and 'wing-like'. **ORDERED**

Scoring: *Allosaurus* = 3 (Madsen 1976); *Coelophysis* = 2 (NMMNH P-42351); *Dilophosaurus* = 3 (UCMP 37302); *Eocursor* = 3 (Butler 2010); *Eucoelophysis* = 2 (NMMNH P-22298); *Heterodontosaurus* = 3 (SAM-K-1332); *Lesothosaurus* = 3 (NHMUK RUB17); *Saturnalia* = 2 (MCP 3844-PV); *Scutellosaurus* = 3 (MNA 175); *Silesaurus* = 2 (ZPAL Ab III/457); *Staurikosaurus* = ?(MCZ 1669); *Velociraptor* = 1 (Norell & Makovicky 1999).

309 – **Scoring**: *Dilophosaurus* = 1 (UCMP 37302); *Eocursor* = 1 (Butler 2010); *Eoraptor* = ?(PVSJ 512); *Pseudolagosuchus* = 1 (PVL 4629); *Scutellosaurus* = 1 (MNA 1752); *Tawa* = 1 (GR 241).

Obs.: state '1' is typical of 'silesaurids' (and highlights the 'notched' condition of their femoral head alluded to in Character 304), but also seen in other basal dinosaurs/dinosauromorphs.

310 – **Scoring**: *Coelophysis* = 0 (NMMNHS 42351); *Eucoelophysis* = 1 (NMMNH P-22298); *Pseudolagosuchus* = ?(PVL 4629); *Saturnalia* = 1 (MCP 3844-PV); *Silesaurus* = 2 (ZPAL Ab III/457), *Tawa* = 1 (GR 241).

311 – **Scoring**: *Dilophosaurus* = 0/1 (UCMP 77270); *Scutellosaurus* = 0/1 (remnant of a shelf is seen on the left side of MNA 1752); *Staurikosaurus* = ?(MCZ 1669).

313 – **Scoring**: *Lagerpeton* = 1 (UNLR 06); *Scutellosaurus* = 0 (MNA 1752).

314 – **Scoring**: *Scutellosaurus* = 1 (MNA 175).

316 – **Scoring**: *Asilisaurus* = 1 (NMT RB19, RB102, RB109, RB112); *Dromomeron gregorii* = 1 (Nesbitt *et al.* 2009a, b); *Eoraptor* = 1 (PVSJ 512); *Eucoelophysis* = 1 (NMMNH P-22298); *Marasuchus* = 1 (PVL 3870, 3871); *Pseudolagosuchus* = 1 (PVL 4629); *Silesaurus* = 1 (ZPAL Ab III/361/23).

Obs.: the fourth trochanter of basal dinosauromorphs may be less expanded than that of most dinosaurs, but is clearly crest shaped and not mound-like.

317 – **Scoring**: *Eucoelophysis* = 0 (NMMNH P-22298); *Staurikosaurus* = ?(MCZ 1669).

324 – **Scoring**: *Asilisaurus* = ?(MNT RB111); *Eucoelophysis* = (NMMNM P-22298); *Pisanosaurus* = ?(PVL 2577); *Pseudolagosuchus* = ?(PVL 4629).

Obs.: it needs to be better defined whether this character refers simply to the area medial to the caudally expanded condyles (in which case nearly all discussed taxa should be scored as '0') or to the proximal extension of that notch, which enters the proximal two-thirds of the femur as a subtle excavation in nearly all discussed taxa.

325 – **Scoring**: *Herrerasaurus* = 1 (Novas 1993).

328 – **Scoring**: *Asilisaurus* = 2 (MNT RB20); *Pisanosaurus* = 1 (PVL 2577); *Silesaurus* = 1/2 (ZPAL Ab III/361/22);

331 – **Scoring**: *Dromomeron romeri* = 1 (Nesbitt *et al.* 2009a, b); *Lagerpeton* = 1 (UNLR 06); *Pisanosaurus* = 1 (PVL 2577).

334 – **Definition**: Tibia, caudolateral flange of the distal portion: (0) absent; (1) present; (2) present and extends well lateral to the craniolateral corner. **ORDERED**

Scoring: *Heterodontosaurus* = ?(SAM-K-1332); *Pisanosaurus* = ?(PVL 2577); *Silesaurus* = 2 (ZPAL Ab III/361/21, 18, 403/1, 411/2, 413, 415, 461); *Tawa* = 2 (GR 242).

335 – **Scoring**: *Scutellosaurus* = 1 (MNA 175).

362 – **Scoring**: *Asilisaurus* = 1 (NMT RB138).

363 – **Scoring**: *Dilophosaurus* = 0 (UCMP 37302); *Herrerasaurus* = 0 (PVSJ 373); *Plateosaurus* = 0 (GPIT 1); *Saturnalia* = 0 (MCP 3844-PV).

366 – **Scoring**: *Allosaurus* = 0 (Madsen 1976); *Dilophosaurus* = 0 (UCMP 37302); *Efraasia* = 0 (SMNS 12354); *Herrerasaurus* = 0 (PVL 2566); *Plateosaurus* = 0 (GPIT 1); *Saturnalia* = 0 (MCP 3844-PV); *Scutelosaurus* = 0 (MNA 1752); *Tawa* = 0 (GR 242).

Obs.: although we agree with Nesbitt (2011) that the astragalus of *Silesaurus* and basal dinosaurs are highly modified, it is clear that the tibial articular facet is not traversed by a laterocaudally-mediocranially oriented ridge, as indeed scored for *Silesaurus* in Nesbitt (2011).

373 – **Scoring**: *Herrerasaurus* = 0 (various specimens; e.g. PVL 2566); *Plateosaurus* = 0 (various specimens; e.g. SMNS 13200); *Silesaurus* = 0 (ZPAL Ab III 361/20).

400 – **Definition**: Pedal unguals: weakly mediolaterally compressed, rounded or triangular in cross section (0); dorsoventrally compressed (1); strongly mediolaterally compressed, with a sharp dorsal keel (2).

Scoring: *Asilisaurus* = 0 (NMT RB146); *Silesaurus* = 0 (ZPAL Ab III/364).

Appendix V

Institutional abbreviations

AMNH, American Museum of Natural History, New York, USA; NHMUK, The Natural History Museum, London, UK; GPIT, Institut und Museum für Geologie und Paläontologie, Universität Tübingen, Germany; GR, Ruth Hall Museum of Paleontology at Ghost Ranch, USA; HMN, Museum für Naturkunde der Humboldt Universität, Berlin, Germany; MCN, Museu de Ciências Naturais, Fundação Zoobotânica do Rio Grande do Sul, Porto Alegre, Brazil; MCP, Museu de Ciências e Tecnologia PUC/RS, Porto Alegre, Brazil; MCZ, Museum of Comparative Zoology, Harvard University, Cambridge, USA; MNA, Museum of Northern Arizona, Flagstaff, USA; NMMNH, New Mexico Museum of Natural History and Science, Albuquerque, USA; NMT, National Museum of Tanzania, Dar es Salaam, Tanzania; PVL, Instituto Miguel Lillo, Tucumán, Argentina; PVSJ, Museo de Ciencias Naturales de la Universidad Nacional de San Juan, San Juan, Argentina; SAM, South African Museum, Cape Town, South Africa; SMNS, Staatliches Museum fur Naturkunde, Stuttgart, Germany; UCMP, University of California Museum of Paleontology, Berkeley, USA; UFRGS, Instituto de Geociências, Universidade Federal do Rio Grande de Sul, Porte Alegre, Brazil; UNLR, Museo de Paleontologia, Universidad Nacional de La Rioja, La Rioja, Argentina; ZPAL, Institute of Paleobiology, Polish Academy of Sciences, Warsaw, Poland.

References

ABDALA, F., RIBEIRO, A. M. & SCHULTZ, C. L. 2001. A rich cynodont fauna of Santa Cruz do Sul, Santa Maria Formation, Middle-Late Triassic), Southern Brazil. *Neues Jahrbuch für Geologie und Paläontologie, Monatshefte*, **2001**, 669–687.

ALLAIN, R. & AQUESBI, N. 2008. Anatomy and phylogenetic relationships of *Tazoudasaurus naimi* (Dinosauria, Sauropoda) from the late Early Jurassic of Morocco. *Geodiversitas*, **30**, 345–424.

ANDREIS, R. R., BOSSI, G. E., MONTARDO, D. K. 1980. O Grupo Rosário do Sul (Triássico) no Rio Grande do Sul. *Anais do XXXI Congresso Brasileiro de Geologia, Camboriú*, SOCIEDADE BRASILEIRA DE GEOLOGIA, **2**, 659–673.

ARCUCCI, A. 1998. New information about dinosaur precursors from the Triassic Los Chañares Fauna, La Rioja, Argentina. *Journal of African Earth Sciences*, **27**, 9–10.

BARBERENA, M. C., ARAÚJO, D. C. & LAVINA, E. L. 1985. Late Permian and Triassic tetrapods of southern Brazil. *National Geographic Research*, **1**, 5–20.

BARRETT, P. M., UPCHURCH, P. & XIAO-LIN, W. 2005. Cranial osteology of *Lufengosaurus huenei* Young (Dinosauria: Prosauropoda) from the Lower Jurassic of Yunnan, People's Republic of China. *Journal of Vertebrate Paleontology*, **25**, 806–822.

BARRETT, P. M., BUTLER, R. J., NOVAS, F. E., MOORE-FAY, S. C., MOODY, J. M., CLARK, J. M. & SÁNCHEZ-VILLAGRA, M. R. 2008. Dinosaur remains from the La Quinta Formation (Lower or Middle Jurassic) of the Venezuelan Andes. *Paläontologische Zeitschrift*, **82**, 163–177.

BENSON, R., BARRETT, P., POWELL, P. & NORMAN, D. 2008. The taxonomic status of *Megalosaurus bucklandii* (Dinosauria, Theropoda) from The Middle Jurassic of Oxfordshire, UK. *Palaeontology*, **51**, 419–424.

BENTON, M. J. 1984. Tooth form, growth, and function in Triassic rhynchosaurs (Reptilia, Diapsida). *Palaeontology*, **27**, 373–776.

BENTON, M. J. & WALKER, A. 2011. *Saltopus*, a dinosauriform from the Upper Triassic of Scotland. *Earth and Environmental Science Transactions of the Royal Society of Edinburgh*, **101**, 285–299.

BENTON, M. J., JUUL, L., STORRS, G. W. & GALTON, P. M. 2000. Anatomy and systematics of the prosauropod dinosaur *Thecodontosaurus antiquus* from the Upper Triassic of southern England. *Journal of Vertebrate Paleontology*, **20**, 77–108.

BITTENCOURT, J. S. & KELLNER, A. W. A. 2009. The anatomy and phylogenetic position of the Triassic dinosaur *Staurikosaurus pricei* Colbert, 1970. *Zootaxa*, **2079**, 1–56.

BITTENCOURT, J. S., DA ROSA, A. A. S., SCHULTZ, C. L. & LANGER, M. C. 2012. Dinosaur remains from the 'Botucaraí Hill' (Caturrita Formation), Late Triassic of south Brazil, and their stratigraphic context. *Historical Biology*. Doi: 10.1080/08912963.2012.694881.

BONAPARTE, J. F. 1981. Descripcion de *Fasolasuchus tenax* y su significado en la sistematica y evolucion de los Thecodontia. *Revista del Museo Argentino de Ciencias Naturales 'Bernardino Rivadavia'*, **3**, 55–101.

BRINKMAN, D. B. & SUES, H.-D. 1987. A staurikosaurid dinosaur from the Upper Triassic Ischigualasto Formation of Argentina and the relationships of the Staurikosauridae. *Palaeontology*, **30**, 493–503.

BRUSATTE, S. L., BUTLER, R. J., SULEJ, T. & NIEDZWIEDZKI, G. 2009. The taxonomy and anatomy of rauisuchian archosaurs from the Late Triassic of Germany and Poland. *Acta Palaeontologica Polonica*, **54**, 221–230.

BRUSATTE, S. L., BENTON, M. J., DESOJO, J. B. & LANGER, M. C. 2010. The higher-level phylogeny of Archosauria (Tetrapoda: Diapsida). *Journal of Systematic Palaeontology*, **8**, 3–47.

BUTLER, R. J. 2005. The 'fabrosaurid' ornithischian dinosaurs of the Upper Elliot Formation (Lower Jurassic) of South Africa and Lesotho. *Zoological Journal of the Linnean Society*, **145**, 175–218.

BUTLER, R. J. 2010. The anatomy of the basal ornithischian dinosaur *Eocursor parvus* from the lower Elliot Formation (Late Triassic) of South Africa. *Zoological Journal of the Linnean Society*, **160**, 648–84.

BUTLER, R. J., PORRO, L. B. & HECKERT, A. B. 2006. A supposed heterodontosaurid tooth from the Rhaetian of Switzerland and a reassessment of the European Late Triassic record of Ornithischia (Dinosauria). *Neues Jahrbuch für Geologie und Paläontologie, Monatshefte*, **10**, 613–633.

BUTLER, R. J., PORRO, L. B. & NORMAN, D. B. 2008. A juvenile skull of the primitive ornithischian dinosaur *Heterodontosaurus tucki* from the 'Stormberg' of southern Africa. *Journal of Vertebrate Paleontology*, **28**, 702–711.

CABREIRA, S. F. 2004. *Placas maxilo-dentárias em rincossauros Hyperodapedon Huxley, 1859. histologia e morfogênese maxilo-dental: nova abordagem*. MSc dissertation, Universidade Federal do Rio Grande do Sul, Porto Alegre.

CABREIRA, S. F., SCHULTZ, C. L., BITTENCOURT, J. S., SOARES, M. B., FORTIER, D. C., SILVA, L. R. & LANGER, M. C. 2011. New stem-sauropodomorph (Dinosauria, Saurischia) from the Triassic of Brazil. *Naturwissenschaften*, **98**, 1035–1040.

CALDWELL, M. W., BUDNEY, L. A. & LAMOUREUX, O. D. 2003. Histology of tooth attachment tissues in the late cretaceous mosasaurid *Platecarpus*. *Journal of Vertebrate Paleontology*, **23**, 622–630.

CARRANO, M. T. 2007. The appendicular skeleton of *Majungasaurus crenatissimus* (Theropoda: Abelisauridae) from the Late Cretaceous of Madagascar. *Society of Vertebrate Paleontology Memoir*, **8**, 163–179.

CARRANO, M. T. & HUTCHINSON, J. R. 2002. The pelvic and hind limb musculature of *Tyrannosaurus rex* (Dinosauria: Theropoda). *Journal of Morphology*, **253**, 207–28.

CARRANO, M. T., SAMPSON, S. D. & FORSTER, C. A. 2002. The osteology of *Masiakasaurus knopfleri*, a small abelisauroid (Dinosauria: Theropoda) from the Late Cretaceous of Madagascar. *Journal of Vertebrate Paleontology*, **22**, 510–34.

CHATTERJEE, S. 1974. A rhynchosaur from the Upper Triassic Maleri Formation of India. *Philosophical Transactions of the Royal Society of London B*, **267**, 209–261.

CHATTERJEE, S. 1978. A primitive parasuchid (phytosaur) reptile from the Upper Triassic Maleri Formation of India. *Palaeontology*, **21**, 83–127.

CHATTERJEE, S. 1984. A new ornithischian dinosaur from the Triassic of North America. *Naturwissenschaften*, **71**, 630–631.

CHATTERJEE, S. 1985. *Postosuchus*, a new thecodontian reptile from the Triassic of Texas and the origin of tyrannosaurs. *Philosophical Transactions of the Royal Society of London B*, **309**, 395–460.

CHATTERJEE, S. 1991. Cranial anatomy and relationships of a new Triassic bird from Texas. *Philosophical Transactions of the Royal Society of London B*, **332**, 277–342.

COLBERT, E. 1981. A primitive ornithischian dinosaur from the Kayenta Formation of Arizona. *Bulletin of the Museum of Northern Arizona*, **53**, 1–61.

COLBERT, E. H. 1989. The Triassic dinosaur Coelophysis. *Bulletin of the Museum of Northern Arizona*, **57**, 1–160.

CROMPTON, A. W. & ATTRIDGE, J. 1986. Masticatory apparatus of the larger herbivores during Late Triassic and Early Jurassic times. *In*: PADIAN, K. (ed.) *The Beginning of the Age of Dinosaurs*. Cambridge University Press, Cambridge, 223–236.

CRISAFULLI, A. & DUTRA, T. L. 2009. *Kaokoxylon zalesskyi* (Sahni) Maheswari en los niveles superiores de la Secuencia Santa Maria 2 (Formación Caturrita), Cuenca de Paraná, Brasil. *GAEA Journal of Geoscience*, **5**, 61–69.

DILKES, D. W. 1998. The Early Triassic rhynchosaur *Mesosuchus browni* and the interrelationships of basal archosauromorph reptiles. *Philosophical Transactions of the Royal Society of London B*, **353**, 501–541.

DILKES, D. W. 2000. Appendicular myology of the hadrosaurian dinosaur *Maiasaura peeblesorum* from the Late Cretaceous (Campanian) of Montana. *Transactions of the Royal Society of Edinburgh: Earth Sciences*, **90**, 87–125.

DZIK, J. 2003. A beaked herbivorous archosaur with dinosaur affinities from the early Late Triassic of Poland. *Journal of Vertebrate Paleontology*, **23**, 556–574.

DZIK, J. & SULEJ, T. 2007. A review of the early triassic krasiejóow biote from Silesia, Poland. *Paleontologia Polonica*, **64**, 3–27.

EDMUND, A. G. 1960. Tooth replacement phenomena in the lower vertebrates. *Royal Ontario Museum, Life Sciences Contributions*, **52**, 1–190.

EDMUND, A. G. 1969. Dentition. *In*: GANS, C., BELLAIRS, A. & PARSONS, T. (eds). *Biology of the Reptilia. Vol. 1, Morphology A*. Academic Press, London, 117–200.

EWER, R. F. 1965. The anatomy of the thecodont reptile *Euparkeria capensis* Broom. *Philosophical Transactions of the Royal Society of London Series B Biological Sciences*, **248**, 379–435.

EZCURRA, M. D. 2006. A review of the systematic position of the dinosauriform archosaur *Eucoelophysis baldwini* Sullivan and Lucas, 1999 from the Upper Triassic of New Mexico, USA. *Geodiversitas*, **28**, 649–684.

EZCURRA, M. D. 2007. The cranial anatomy of the coelophysoid theropod *Zupaysaurus rougieri* (Upper Triassic, Argentina). *Historical Biology*, **19**, 185–202.

FERIGOLO, J. & LANGER, M. C. 2006. The origin of the ornithischian predentary bone. *Journal of Vertebrate Paleontology*, **25**(supplement to 3), 56A.

FERIGOLO, J. & LANGER, M. C. 2007. A Late Triassic dinosauriform from south Brazil and the origin of the ornithischian predentary bone. *Historical Biology*, **19**, 23–33.

FORSTER, C. A., FARKE, A. A., MCCARTNEY, J. A., DE KLERK, W. J. & ROSS, C. F. 2009. A 'Basal' Tetanuran from the Lower Cretaceous Kirkwood Formation of South Africa. *Journal of Vertebrate Paleontology*, **29**, 283–285.

FOSTOWICZ-FRELIK, L. & SULEJ, T. 2010. Bone histology of *Silesaurus opolensis* Dzik, 2003 from the Late Triassic of Poland. *Lethaia*, **43**, 137–148.

FRASER, M. & SUES, H.-D. 2011. The beginning of the 'Age of Dinosaurs': a brief overview of terrestrial biotic changes during the Triassic. *Earth and Environmental Science Transactions of the Royal Society of Edinburgh*, **101**, 189–200.

Fraser, N., Padian, K., Walkden, G. & Davis, A. 2002. Basal dinosauriform remains from Britain and the diagnosis of the Dinosauria. *Palaeontology*, **45**, 79–95.

Furin, S., Preto, N., Rigo, M., Roghi, G., Gianolla, P., Crowley, J. L. & Bowring, S. A. 2006. High-precision U–Pb zircon age from the Triassic of Italy: implications for the Triassic time scale and the Carnian origin of calcareous nannoplankton and dinosaurs. *Geology*, **34**, 1009–1012.

Gallego, O. F. 1996. Revisión de algunos conchostracos de la Formación Santa Maria (Triásico Medio) de Rio Grande do Sul (Brasil). *Acta Geologica Leopoldensia*, **19**, 59–76.

Galton, P. M. 1974. The ornithischian dinosaur *Hypsilophodon* from the Wealden of the Isle of Wight. *Bulletin of the British Museum of Natural History*, **25**, 1–152.

Galton, P. M. 1978. Fabrosauridae, the basal family of ornithis-chian dinosaurs (Reptilia: Ornithopoda). *Paliontologische Zeitschrift*, **52**, 138–159.

Galton, P. M. 2005. Bones of large dinosaurs (Prosauropoda and Stegosauria) from the Rhaetic Bone Bed (Upper Triassic) of Aust Cliff, southwest England. *Revue de Paléobiologie*, **24**, 51–74.

Galton, P. M. & Walker, A. 1996. Supposed prosauropod dinosaurs from Middle Triassic of England referred to Parasauchia and Dinosauriformes. *Neues Jarhbuch füur Geologie und Paläontologie Monatshefte*, **1996**, 727–738.

Gauffre, F.-X. 1993. The prosauropod dinosaur *Azendohsaurus laaroussi* from the Upper Triassic of Morocco. *Palaeontology*, **36**, 897–908.

Goloboff, P., Farris, J. & Nixon, K. 2008. TNT, a free program for phylogenetic analysis. *Cladistics*, **24**, 774–786.

Gow, C. E., Kitching, J. W. & Raath, M. A. 1990. Skulls of the prosauropod dinosaur *Massospondylus carinatus* Owen in the collections of the Bernard Price Institute for Palaeontological Research. *Palaeontologia Africana*, **27**, 45–58.

Gower, D. J. 1999. The cranial and mandibular osteology of a new rauisuchian archosaur from the Middle Triassic of southern Germany. *Stuttgarter Beiträage zur Naturkunde B*, **280**, 1–49.

Gower, D. J. & Sennikov, A. G. 1997. *Sarmatosuchus* and the early history of the Archosauria. *Journal of Vertebrate Paleontology*, **17**, 60–73.

Guerra-Sommer, M. & Cazzulo-Klepzig, M. 2000. The Triassic taphoflora from Parana Basin, southern Brazil: an overview. *Revista Brasileira de Geologia*, **30**, 481–485.

Haubold, H. 1991. Ein neuer Dinosaurier (Ornithischia, Thyreophora) aus dem unteren Jura des nöordlichen Mitteleuropa. *Revue de Paléobiologie*, **9**, 149–177.

Heerden, J. van. 1979. The morphology and taxonomy of *Euskelosaurus* (Reptilia: Saurischia: Late Triassic) from South Africa. *Navorsinge Van Die Nasionale Museum Bloemfontein*, **4**, 21–84.

Holz, M. & Scherer, C. 2000. Sedimentological and paleontological evidence of paleoclimatic change during the South Brazilian Triassic: the register of a global trend towards a humid paleoclimate. *Zentralblatt für Geologie und Paläontologie (Teil I)*, **11–12**, 1589–1609.

Hopson, J. A. 1975. On the generic separation of the ornithischian dinosaurs *Lycorhinus* and *Heterodontosaurus* from the Stormberg Series (Upper Triassic) of South Africa. *South African Journal of Science*, **71**, 302–305.

Huene, F. von 1926. Vollständige Osteologie eines Plateosauriden aus dem schwäbischen Keuper. *Geologie und Paläontologie Abhandlungen (Neue Folge)*, **15**, 139–179.

Huene, F. von 1942. *Die fossilen Reptilien des Süudamerikanischen Gondwanalandes*. C. H. Beckscke Verlag, Munich.

Hutchinson, J. R. 2001. The evolution of the pelvic osteology and soft tissues on the line to extant birds (Neornithes). *Zoological Journal of the Linnean Society*, **131**, 123–168.

Irmis, R. B. 2011. Evaluating hypotheses for the early diversification of dinosaurs. *Earth and Environmental Science Transactions of the Royal Society of Edinburgh*, **101**, 397–428.

Irmis, R. B., Nesbitt, S. J., Padian, K., Smith, N. D., Turner, A. H., Woody, D. & Downs, A. 2007a. A Late Triassic dinosauromorph assemblage from New Mexico and the rise of dinosaurs. *Science*, **317**, 358–361.

Irmis, R. B., Parker, W. G., Nesbitt, S. J. & Liu, J. 2007b. Early ornithischian dinosaurs: the Triassic record. *Historical Biology*, **19**, 3–22.

Irmis, R. B., Mundil, R., Martz, J. W. & Parker, W. G. 2011. High-resolution U-Pb ages from the Upper Triassic Chinle Formation (New Mexico, USA) support a diachronous rise of dinosaurs. *Earth and Planetary Science Letters*, **309**, 258–267.

Jalil, N.-E. & Peyer, K. 2007. A new rauisuchian (Archosauria, Suchia) from the Upper Triassic of the Argana Basin, Morocco. *Palaeontology*, **50**, 417–430.

Kammerer, C., Nesbitt, S. J. & Shubin, N. H. 2012. The first basal dinosauriform (Silesauridae) from the Late Triassic of Morocco. *Acta Paleontologica Polonica*, **57**, 277–284.

Kutty, T. S., Chatterjee, S., Galton, P. M. & Upchurch, P. 2007. Basal sauropodomorphs (Dinosauria: Saurischia) from the Lower Jurassic of India: their anatomy and relationships. *Journal of Paleontology*, **81**, 1218–1240.

Langer, M. C. 2003. The sacral and pelvic anatomy of the stem-sauropodomorph Saturnalia tupiniquim (Late Triassic, Brazil). *Paleobios*, **23**, 1–40.

Langer, M. C. 2004. Basal Saurischia. *In*: Weishampel, D. B., Dodson, P. & Osmólska, H. (eds) *The Dinosauria. 2nd edition*. University of California Press, Berkley, 25–46.

Langer, M. C. & Benton, M. J. 2006. Early dinosaurs: A phylogenetic study. *Journal of Systematic Palaeontology*, **4**, 309–358.

Langer, M. C., Ribeiro, A. M., Schultz, C. L. & Ferigolo, J. 2007. The continental tetrapod-bearing Triassic of south Brazil. *New Mexico Museum of Natural History and Science Bulletin*, **41**, 201–218.

Langer, M. C., Ezcurra, M. D., Bittencourt, J. S. & Novas, F. E. 2010. The origin and early evolution of dinosaurs. *Biological Reviews*, **85**, 55–110.

Langer, M. C., Bittencourt, J. S. & Schultz, C. L. 2011. A reassessment of the basal dinosaur

Guaibasaurus candelariensis, from the Late Triassic Caturrita Formation of south Brazil. *Earth and Environmental Science Transactions of the Royal Society of Edinburgh*, **101**, 301–332.

LUCAS, S. G. 2001. Age and correlation of Triassic tetrapod assemblages from Brazil. *Albertiana*, **26**, 13–20.

MADSEN, J. H. 1976. Allosaurus Fragilis: A Revised Osteology. *Utah Geological Survey Bulletin*, **109**, 1–163.

MADSEN, J. H. & WELLES, S. P. 2000. Ceratosaurus *(Dinosauria, Theropoda): A Revised Osteology*. Utah Geological Survey Miscellaneous Publications, Salt Lake City.

MARTIN, L. 1981. Mesozoic birds and the origin of birds. *In*: SCHULTZE, H,-P. & TRUEB, L. (eds) *Origins of the Higher Groups of Tetrapods. Controversy and Consensus*. Cornell University Press, Comstock, 485–540.

MARTÍNEZ, R. N. 2009. *Adeopapposaurus mognai, gen*. et sp. nov. (Dinosauria: Sauropodomorpha), with comments on adaptations of basal Sauropodomorpha. *Journal of Vertebrate Paleontology*, **29**, 142–164.

MARTINEZ, R. N. & ALCOBER, O. A. 2009. A basal sauropodomorph (Dinosauria: Saurischia) from the Ischigualasto Formation (Triassic, Carnian) and the early evolution of Sauropodomorpha. *PLoS One*, **4**, 4391–4312.

MARTINEZ, R. N., SERENO, P. C., ALCOBER, O. A., COLOMBI, C. E., RENNE, P. R., MONTAÑEZ, I. P. & CURRIE, B. S. 2011. A basal dinosaur from the dawn of the dinosaur era in southwestern Pangaea. *Science*, **331**, 206–210.

MOCZEK, A. P. 2008. On the origins of novelty in development and evolution. *BioEssays*, **30**, 432–447.

MODESTO, S. P. & SUES, H.-D. 2004. The skull of the Early Triassic archosauromorph reptile *Prolacerta broomi* and its phylogenetic significance. *Zoological Journal of the Linnean Society*, **140**, 335–351.

MOTANI, R. 1997. Temporal and spatial distribution of tooth implantation in ichthyosaurs. *In*: CALLAWAY, J. M & NICHOLLS, E. L. (eds) *Ancient Marine Reptiles*. Academic Press, London, 81–103.

MÜLLER, G. B. & WAGNER, G. P. 1991. Novelty in evolution: Restructuring the concept. *Annual Review of Ecology and Systematics*, **22**, 229–256.

MUTTONI, G., KENT, D. V., OLSEN, P. E., DI STEFANO, P., LOWRIE, W., BERNASCONI, S. M. & HERNANDEZ, F. M. 2004. Tethyan magnetostratigraphy from Pizzo Mondello (Sicily) and correlation to the Late Triassic Newark astrochronological polarity time scale. *Geological Society of America Bulletin*, **116**, 1043–1058.

NESBITT, S. J. 2007. The anatomy of *Effigia okeeffeae* (Archosauria, Suchia), theropod convergence, and the distribution of related taxa. *Bulletin of the American Museum of Natural History*, **302**, 1–84.

NESBITT, S. J. 2011. The early evolution of Archosauria: relationships and the origin of major clades. *Bulletin of the American Museum of Natural History*, **352**, 1–292.

NESBITT, S. J., IRMIS, R. B. & PARKER, W. G. 2007. A critical reevaluation of the Late Triassic dinosaur taxa of North America. *Journal of Systematic Palaeontology*, **5**, 209–243.

NESBITT, S. J., SMITH, N. D., IRMIS, R. B., TURNER, A. H., DOWNS, A. & NORELL, M. A. 2009a. A complete skeleton of a Late Triassic saurischian and the early evolution of dinosaurs. *Science*, **326**, 1530–1533.

NESBITT, S. J., IRMIS, R. B., PARKER, W. G., SMITH, N. D., TURNER, A. H. & ROWE, T. 2009b. Hindlimb osteology and distribution of basal dinosauromorphs from the Late Triassic of North America. *Journal of Vertebrate Paleontology*, **29**, 498–516.

NESBITT, S. J., SIDOR, C. A., IRMIS, R. B., ANGIELCZYK, K. D., SMITH, R. M. H. & TSUJI, L. A. 2010. Ecologically distinct dinosaurian sister-group shows early diversification of Ornithodira. *Nature*, **464**, 95–98.

NIEDZWIEDZKI, G., PIECHOWSKI, R. & SULEJ, T. 2009. New data on the anatomy and phylogenetic position of *Silesaurus opolensis* from the late Carnian of Poland. *Journal of Vertebrate Paleontology*, **29** (Suppl 3), 155A.

NORELL, M. A. & HWANG, S. H. 2004. A Troodontid Dinosaur from Ukhaa Tolgod (Late Cretaceous Mongolia). *American Museum Novitates*, **3446**, 1–9.

NORELL, M. A. & MAKOVICKY, P. J. 1999. Important features of the dromaeosaurid skeleton II: information from newly collected specimens of *Velociraptor mongoliensis*. *American Museum Novitates*, **3282**, 1–45.

NORMAN, D. B., BUTLER, R. J. & MAIDMENT, S. C. H. 2007. Reconsidering the status and affinities of the ornithischian dinosaur *Tatisaurus oehleri* Simmons, 1965. *Zoological Journal of the Linnean Society*, **150**, 865–874.

NORMAN, D. B., CROMPTON, A. W., BUTLER, R. J., PORRO, L. B. & CHARIG, A. J. 2011. The Lower Jurassic ornithischian dinosaur *Heterodontosaurus tucki* Crompton & Charig, 1962: cranial anatomy, functional morphology, taxonomy, and relationships. *Zoological Journal of the Linnean Society*, **163**, 182–276.

NOVAS, F. E. 1993. New information on the systematics and postcranial skeleton of *Herrerasaurus ischigualastensis* (Theropoda: Herrerasauridae) from the Ischigualasto Formation (Upper Triassic) of Argentina. *Journal of Vertebrate Paleontology*, **13**, 400–423.

NOVAS, F. E. 1996. Dinosaur monophyly. *Journal of Vertebrate Paleontology*, **16**, 723–741.

NOVAS, F. E., EZCURRA, M. D., CHATTERJEE, S. & KUTTY, T. S. 2011. New dinosaur species from the Upper Triassic Upper Maleri and Lower Dharmaran formations of central India. *Earth and Environmental Science Transactions of the Royal Society of Edinburgh*, **101**, 333–350.

OLSEN, P. E., KENT, D. V. & WHITESIDE, J. H. 2011. Implications of the Newark Supergroup-based astrochronology and geomagnetic polarity tyime scale (Newark-APTS) for the tempo and mode of the early diversification of the Dinosauria. *Earth and Environmental Science Transactions of the Royal Society of Edinburgh*, **101**, 201–229.

OSBORN, J. W. 1984. From reptile to mammal: evolutionary considerations of the dentition with emphasis on tooth attachment. *Symposium of the Zoological Society of London*, **52**, 549–574.

PADIAN, K. 1986. On the type material of *Coelophysis* Cope (Saurischia: Theropoda) and a new specimen from the Petrified Forest of Arizona (Late Triassic: Chinle Formation). In PADIAN, K. (ed.) *The Beginning of the Age of Dinosaurs*. Cambridge University Press, Cambridge, 45–60.

PARKER, W. G., IRMIS, R. B. & NESBITT, S. J. 2006. Review of the Late Triassic dinosaur record from Petrified Forest National Park, Arizona. *Museum of Northern Arizona Bulletin*, **62**, 160–161.

PEECOOK, B., SIDOR, C., NESBITT, S. & ANGIELCZYK, K. 2011. New data on the archosaur fauna of the Middle Triassic (Anisian) Ntawere Formation of Zambia. *Journal of Vertebrate Paleontology*, **31**, 172.

PEREZ, P. A. & MALABARBA, M. C. 2002. A Triassic freshwater fish fauna from the Paraná Basin in southern Brazil. *Revista Brasileira de Paleontologia*, **4**, 27–33.

PIECHOWSKI, R. & DZIK, J. 2010. The axial skeleton of Silesaurus opolensis. *Journal of Vertebrate Paleontology*, **30**, 1127–1141.

DE PINNA, M. C. C. 1991. Concepts and tests of homology in the cladistic paradigm. *Cladistics*, **7**, 367–394.

PINTO, I. D. 1956. Artrópodos da Formação Santa Maria (Triássico Superior) do Rio Grande do Sul, com notícias sobre alguns restos vegetais. *Boletim da Sociedade Brasileira de Geologia*, **5**, 75–87.

POL, D., RAUHUT, O. W. M. & BECERRA, M. 2011. A Middle Jurassic heterodontosaurid dinosaur from Patagonia and the evolution of heterodontosaurids. *Naturwissenschaften*, **98**, 369–379.

RAATH, M. 1977. *The anatomy of the Triassic theropod* Syntarsus rhodesiensis *(Saurischia: Podokesauridae) and a consideration of its biology*. PhD dissertation, Rhodes University, Salisbury.

RAATH, M. 1990. Morphological variation in small theropods and its meaning in systematics: Evidence from *Syntarsus rhodesiensis*. *In*: CARPENTER, K. & CURRIE, P. J. (eds) *Dinosaur Systematics: Approaches and Perspectives*. Cambridge University Press, Cambridge, 91–105.

RAUHUT, O. W. M. 2003. The interrelationships and evolution of basal theropod dinosaurs. *Special Papers in Palaeontology*, **69**, 1–213.

RAUHUT, O. W. M. 2005. Osteology and relationships of a new theropod dinosaur from the Middle Jurassic of Patagonia. *Palaeontology*, **48**, 87–110.

RAUHUT, O. W. M & FECHNER, R. 2005. Early development of the facial region in a non-avian theropod dinosaur. *Proceedings of the Royal Society London B*, **272**, 1179–1183.

REMANE, A. 1952. *Die Grundlagen des natürlichen Systems der vergleichended Anatomie and the Phylogenetik*. Geest und Portig, Leipzig.

REMES, K. 2007. *Evolution of the pectoral girdle and forelimb in Sauropodomorpha (Dinosauria, Saurischia): osteology, myology and function*. PhD dissertation, Ludwigs Maximilians Universität, München.

RIBEIRO, A. M., ABDALA, N. F. & BERTONI, R. S. 2011. Traversodontid cynodonts (Therapsida-Eucynodontia) from two upper Triassic localities of the Paraná Basin, southern Brazil. *Abstracts of the 4th Congreso Latinoamericano de Paleontología de Vertebrados*, San Juan, 375.

RIEPPEL, O. & KEARNEY, M. 2002. Similarity. *Biological Journal of the Linnean Society*, **75**, 59–82.

ROSENBAUM, J. N. & PADIAN, K. 2000. New material of the basal thyreophoran *Scutellosaurus lawleri* from the Kayenta Formation (Lower Jurassic) of Arizona. *PaleoBios*, **20**, 13–23.

ROWE, T. 1989. A new species of the theropod dinosaur *Syntarsus* from the Early Jurassic Kayenta Formation of Arizona. *Journal of Vertebrate Paleontology*, **9**, 125–136.

SÄILÄ, L. K. 2009. Alpha taxonomy of the Russian Permian procolophonoid reptiles. *Acta Palaeontologica Polonica*, **54**, 599–608.

SAMPSON, S. D. & WITMER, L. M. 2007. Craniofacial anatomy of *Majungasaurus crenatissimus* (Theropoda: Abelisauridae) from the Late Cretaceous of Madagascar. *Journal of Vertebrate Paleontology*, **27**, 32–102.

SANTA LUCA, A. P. 1980. The postcranial skeleton of *Heterodontosaurus tucki* (Reptilia, Ornithischia) from the Stormberg of South Africa. *Annals of South African Museum*, **79**, 159–211.

SCHULTZ, C. L., SCHERER, C. M. S. & BARBERENA, M. C. 2001. Biostratigraphy of southern Brazilian Middle-Upper Triassic. *Revista Brasileira de Geociências*, **30**, 491–494.

SERENO, P. C. 1991. Basal archosaurs: phylogenetic relationships and functional implications. *Memoir of the Society of Vertebrate Paleontology*, **2**, 1–53.

SERENO, P. C. 1993. The pectoral girdle and forelimb of the basal theropod *Herrerasaurus ischigualastensis*. *Journal of Vertebrate Paleontology*, **13**, 425–450.

SERENO, P. C. 1999. The evolution of dinosaurs. *Science*, **284**, 2137–2147.

SERENO, P. C. 2007. The phylogenetic relationships of early dinosaurs: a comparative report. *Historical Biology*, **19**, 145–155.

SERENO, P. C. & DONG, Z.-M. 1992. The skull of the basal stegosaur *Huayangosaurus taibaii* and a cladistic diagnosis of Stegosauria. *Journal of Vertebrate Paleontology*, **51**, 318–343.

SERENO, P. C. & ARCUCCI, A. B. 1994a. Dinosaurian precursors from the Middle Triassic of Argentina: *Lagerpeton chanarensis*. *Journal of Vertebrate Paleontology*, **13**, 385–399.

SERENO, P. C. & ARCUCCI, A. B. 1994b. Dinosaurian precursors from the Middle Triassic of Argentina: *Marasuchus lilloensis*, gen. *nov*. *Journal of Vertebrate Paleontology*, **14**, 53–73.

SERENO, P. C. & BRUSATTE, S. L. 2008. Basal abelisaurid and carcharodontosaurid theropods from the Lower Cretaceous Elrhaz Formation of Niger. *Acta Palaeontologica Polonica*, **53**, 15–46.

SMALL, B. J. 1997. A new procolophonid from the Upper Triassic of Texas, with a description of tooth replacement and implantation. *Journal of Vertebrate Palaeontology*, **17**, 674–678.

SMALL, B. 2009. A Late Triassic dinosauromorph assemblage from the Eagle Basin (Chinle Formation), Colorado, U.S.A. *Journal of Vertebrate Paleontology*, **29**, 182A.

SOARES, M. B., ABDALA, F. & BERTONI-MACHADO, C. 2011a. A sectorial toothed cynodont (Therapsida) from the Triassic Santa Cruz do Sul fauna, Santa Maria Formation, Southern Brazil. *Geodiversitas*, **33**, 265–278.

SOARES, M. B., SCHULTZ, C. L. & HORN, B. 2011b. New information on *Riograndia guaibensis* Bonaparte, Ferigolo & Ribeiro, 2001 (Eucynodontia, Tritheledontidae) from the Late Triassic of southern Brazil:

anatomical and biostratigraphic implications. *Anais da Academia Brasileira de Ciências*, **83**, 329–354.

SUES, H.-D. 2003. An unusual new archosauromorph reptile from the Upper Triassic Wolfville Formation of Nova Scotia. *Canadian Journal of Earth Sciences*, **40**, 635–649.

SULEJ, T., BRONOWICZ, R., TAŁANDA, M. & NIEDŹWIEDZKI, G. 2011. A new dicynodont-archosaur assemblage from the Late Triassic (Carnian) of Poland. *Earth and Environmental Science Transactions of the Royal Society of Edinburgh*, **101**, 261–269.

SULLIVAN, R. M. & LUCAS, S. G. 1999. Eucoelophysis baldwini, a new theropod dinosaur from the Upper Triassic of New Mexico, and the status of the original types of Coelophysis. *Journal of Vertebrate Paleontology*, **19**, 81–90.

THULBORN, R. A. 1970. The skull of *Fabrosaurus australis*, a Triassic ornithischian dinosaur. *Palaeontology*, **13**, 414–432.

THULBORN, R. A. 1972. The post-cranial skeleton of the Triassic ornithischian dinosaur *Fabrosaurus australis*. *Palaeontology*, **15**, 29–60.

THULBORN, R. A. 1974. A new heterodontosaurid dinosaur (Reptilia:Ornithischia) from the Upper Triassic Red Beds of Lesotho. *Zoological Journal of the Linnean Society*, **55**, 151–175.

THULBORN, R. A. 1992. Taxonomic characters of *Fabrosaurus australis*, an ornithischian dinosaur from the Lower Jurassic of southern Africa. *Geobios*, **25**, 283–292.

TYKOSKI, R. 2005. *Osteology, ontogeny, and relationships of the coelophysoid theropods*. PhD thesis, The University of Texas, Austin.

TYKOSKI, R. S. & ROWE, T. 2004. Ceratosauria. *In*: WEISHAMPEL, D. B., DODSON, P. & OSMÓLSKA, H. (eds) *The Dinosauria. 2nd edition*. University of California Press, Berkley, 47–70.

UPCHURCH, P., BARRETT, P. M., ZHAO, X. & XU, X. 2007. A re-evaluation of *Chinshakiangosaurus chunghoensis* Ye *vide* Dong 1992 (Dinosauria Sauropodomorpha): implications for cranial evolution in basal sauropod dinosaurs. *Geological Magazine*, **144**, 247–262.

WALKER, A. D. 1990. A revision of *Sphenosuchus acutus* Haughton, crocodylomorph reptile from the Elliot Formation (Late Triassic or Early Jurassic) of South Africa. *Philosophical Transactions of the Royal Society of London B Biological Sciences*, **330**, 1–120.

WELLES, S. P. 1984. Dilophosaurus wetherilli (Dinosauria, Theropoda): osteology and comparisons. *Palaeontographica Abteilung A*, **185**, 85–180.

WILEY, E. O. 1975. Karl R. Popper, systematics, and classification: a reply to Walter Bock and other evolutionary taxonomists. *Systematic Zoology*, **24**, 233–243.

WITMER, L. M. 1997. The evolution of the antorbital cavity of archosaurs: a study in soft-tissue reconstruction in the fossil record with an analysis of the function of pneumaticity. *Society of Vertebrate Paleontology, Memoir*, **3**, 1–73.

YATES, A. M. 2003. A new species of the primitive dinosaur, Thecodontosaurus (Saurischia: Sauropodomorpha), and its implications for the systematics of early dinosaurs. *Journal of Systematic Palaeontology*, **1**, 1–42.

YATES, A. M. 2005. A new theropod dinosaur from the Early Jurassic of South Africa and its implication for the early evolution of theropods. *Palaeontologia Africana*, **41**, 105–122.

ZERFASS, H. 2007. *Geologia da Folha Agudo, SH.22-V-C-V, escala 1:100.000*. Serviço. Geológico do Brasil – CPRM, Porto Alegre.

ZERFASS, H., LAVINA, E. L., SCHULTZ, C. L., GARCIA, A. G. V., FACCINI, U. F. & CHEMALE, F., JR. 2003. Sequence stratigraphy of continental Triassic strata of southernmost Brazil: a contribution to Southwestern-Gondwana palaeogeography and palaeoclimate. *Sedimentary Geology*, **161**, 85–180.

ZERFASS, H., CHEMALE, F., JR., SCHULTZ, C. L. & LAVINA, E. L. 2004. Tectonics and sedimentation in Southern South America during Triassic. *Sedimentary Geology*, **166**, 265–292.

ZHENG, X.-T., YOU, H.-L., XU, X. & DONG, Z.-M. 2009. An Early Cretaceous heterodontosaurid dinosaur with filamentous integumentary structures. *Nature*, **458**, 333–336.